DOWN-TO-EARTH STUDIES OF CARBON CLUSTERS *

R. E. Smalley

Rice University

ABSTRACT

Recent advances in supersonic beam experiments with laser-vaporization sources of clusters have provided some interesting new insights into the nature of the small clusters of carbon, and the processes through which carbon condenses. One cluster in particular, C_{60}, appears to play a central role. It is argued that this cluster takes the shape of a soccerball: a hollow sphere composed of a shell of 60 carbon atoms connected by a lattice of hexagonal and pentagonal rings, in a pattern of overall icosahedral symmetry. Although C_{60} appears to be uniquely stable due to its perfect symmetry, all other even-numbered carbon clusters in the 32-100+ atom size range seem to favor similar closed spheroidal forms. These species are interpreted as relatively unreactive side products in condensation reactions of carbon vapor involving spiraling graphitic sheets. The prevalence of C_{60} in laser-vaporized carbon vapors and sooting flames suggests that it may be formed readily whenever carbon condenses. Such ready formation and extraordinary stability may have substantial astrophysical implications.

I. INTRODUCTION

Development of laser techniques with supersonic molecular beams has stimulated a flurry of new results from earth-based, laboratory measurements on carbon. Although these new results are still in the process of verification, extension, and further interpretation, a rather remarkable new picture is beginning to emerge as to the processes of carbon condensation and the nature of the species involved. Perhaps the most concise way to introduce this subject is simply to list the key features of this new picture.

(1) Carbon nucleates to form small clusters far more readily than any other element in the periodic table (including such refractory elements as tungsten and tantalum).

(2) The smallest clusters (C_2 through C_9) are most stable in the form of linear chains.

----

(3) Clusters in the 10-29 atom size range take the form of monocyclic rings.

(4) Even-numbered clusters in the 32--100+ atom size range take the form of closed spheroidal shells (the "fullerenes").

(5) Odd-numbered clusters in the 33-101+ atom size range take the form of nearly-closed spheroidal shells (the "semifullerenes").

(6) C_{60} ("buckminsterfullerene") prefers the shape of a soccerball. Because of its size and perfect symmetry, it is extremely stable (chemically, thermodynamically, photophysically).

(7) A spiral shell is a good model for the active nucleus involved in carbon grain growth (and soot formation).

(8) The fullerenes are side products (dead ends) in the process of soot formation.

(9) The fullerenes are made whenever carbon condenses, including sooting flames.

(10) Metal atoms may be trapped inside completely closed fullerene shells.

When compared to the view prevalent in the carbon literature only a few years ago, these 10 points (with the possible exception of the first two or three) are quite divergent. Nonetheless, my colleagues and I have found the new experimental evidence compelling. To our knowledge this picture is the only one consistent with all experimental results, both new and old. This is intellectually quite an exciting time in carbon cluster research since in many essential aspects the new view is still rather controversial. We believe the evidence is strong, although in a few remaining cases the definitive experiment has yet to be done.

In most areas of cluster science new insights and observations are of fairly esoteric interest. But carbon is special. If the above points are correct there are major implications both in the fields of combustion and astrophysics. So it is well to review what is now quite an extensive body of experimental evidence, and let each observer come to her/his own conclusions.

II. LASER VAPORIZATION CLUSTER BEAMS & ABUNDANCE DISTRIBUTIONS

Figure 1 shows a schematic of the sort of laser- vaporization cluster source used for the new carbon cluster experiments. This new technique was developed at Rice particularly for the study of small clusters of transition metals, but turned out to be rather general in scope (refs. 1-4). Here a pulsed laser is directed at the surface of the material to be studied. With currently available pulsed lasers one can easily generate temperatures on the target material in excess of 10,000K in this apparatus, readily vaporizing any known substance in such a short period of time that the rest of the source can operate at room temperature. The cool,

high density helium flowing over the target then serves as a buffer gas in which clusters of the target material form, thermalize to near room temperature, and then cool to near 0 K in the subsequent supersonic expansion as this helium emerges into a well-pumped vacuum chamber. Collimated beams skimmed from these supersonic cluster expansions then provide useful sources for detailed study of a vast set of fascinating new cluster species.

The first such experiment on carbon was performed by a group at Exxon (ref. 5) using an apparatus originally developed and built at Rice. As shown in Figure 2, a rather dramatic result is obtained in such an apparatus: there are two distinct cluster distributions. In the higher mass distribution only even-numbered clusters are observed. The Exxon group was uncertain as to the reason for the prominence of this second, even-numbered distribution, although they suggested it may be evidence for the formation during vaporization of a hypothetical "carbyne" form of carbon consisting of linear chains of triply-bonded carbon, much as had been reported previously (see ref. 6 and references therein). As it turned out, the real reason for this bizarre bimodal distribution appears to be even more interesting.

The key to unraveling this mystery appeared in experiments at Rice in the late summer of 1985 while my colleagues and I were exploring the chemical reactivity of the smaller-sized side of the bimodal carbon cluster distribution. Incidentally we noticed that one particular member of the large cluster distribution, C_{60}, often appeared significantly more intense in the supersonic beam than any other. Upon further study we found that the relative abundance of this special cluster was sensitive to the detailed clustering and reaction conditions in the supersonic nozzle (ref. 7). This is most clearly seen in Figure 3, which compares the cluster distribution obtained under two extremes. In each the abundance of each cluster is being monitored as a function of cluster size by direct 1-photon ionization with an F_2 excimer laser (photon energy 7.9 eV) followed by time-of-flight (TOF) mass analysis of the cluster photoions. The bottom half of Fig. 3 shows the TOF spectrum of the clusters made by laser vaporization very early in the supersonic gas pulse when there is very little helium buffer gas present over the graphite target. Ordinarily under these conditions very little if any clusters are produced -- even with such refractory elements as tungsten, molybdenum, tantalum, and platinum. But carbon is by far the most facile at cluster formation of any element we have yet examined in such an apparatus. As shown in the bottom panel of Figure 3 these mild clustering conditions readily produce an abundance of large clusters of carbon. Note that there is no significant even-odd alternation in abundance, and no single cluster dominates the distribution.

However, the top panel of Figure 3 shows that a dramatic change in the cluster distribution occurs when more extreme clustering conditions are used in the nozzle. Here the vaporization laser was fired at the peak of the helium carrier gas pulse, when the effective helium pressure above the graphite target was roughly 1 atmosphere. At this higher pressure the laser-induced carbon vapor plume in more rapidly cooled, it is more effectively confined to a small volume in flowing gas during the subsequent passage out the rest of the supersonic nozzle, and diffusional loss to the nozzle walls is minimized. The result is that these high-pressure nozzle conditions are far more conducive to cluster growth, both by carbon atom addition and by reaction with small carbon radicals. In order to push this cluster growth and aging process to an extreme, a small reservoir was added to the down-stream section of the nozzle to prolong the reaction time prior to

formation of the free supersonic expansion. As shown by the top panel of Fig 3, these extreme clustering conditions leave primarily just one cluster behind in this size range: the remarkable C_{60}.

To us the most striking aspect of this prominence of C_{60} was the fact that none of the clusters of similar mass showed any suggestion that a particularly stable cluster was nearby: clusters of 52,54,56,58,62,64,68 carbon atoms all seemed to behave about the same. Upon a bit of reflection it occurred to us that this may be due to the fact that 60 is the number of vertices of a truncated icosahedron (ie. a soccer ball). Carbon with such a bonding structure would have its bonding needs met in a beautifully symmetrical fashion. The direct correspondence of this figure and the geodesic domes of R. Buckminsterfuller led us to suggest the rather tortuous name of "buckminsterfullerene" for this hypothetical form of carbon (ref. 7).

The likely stability of such a spheroidal 60-atom molecule of carbon had in fact been predicted before the new beam experiments (refs 8-10). In the two years since our original realization of the special aspect of C_{60}, a flood of calculations have appeared with successively higher level predictions of the stability and electronic structure of this icosahedral form of carbon (refs 11-40). Regardless of the theoretical approach used, there is now general agreement that this structure for C_{60} should be expected to result in a strongly bound, electronically closed shell, highly stable molecule.

III. REACTIVITY STUDIES

Shortly after the initial realization that C_{60} was very special, and an early indication that a metal atom such as lanthanum could be put inside its spheroidal cage (ref. 41), we used a rapid flow reactor technique (ref. 42) to measure the reactivity of these carbon clusters toward various reagents (ref. 43). The principal result of this study is shown in Figure 4. Here again the TOF mass spectrum is shown of carbon cluster species in the supersonic beam as probed by direct photoionization with an F_2 excimer laser. The top mass spectrum is a control showing the cluster distribution prior to reaction, the bottom panel shows the mass spectrum obtained after a flow of nitric oxide (NO) had been added to the fast-flow reactor. Under the conditions used the average carbon cluster received on the order of 10,000 potential reactive hard sphere collisions with the NO reactant molecules during passage at near 300 K through the reactor.

As expected, C_{60} was found to be effectively inert under these reaction conditions even with such active reagents as NO, SO_2, O_2, NH_3, and H_2O. As can be readily seen in Fig. 4, the odd-numbered clusters, and all clusters smaller than C_{36} were found to react readily -- just as would be expected if these species possessed one or more active carbon sites with effectively "dangling" bonds. The most striking result, however, was that not only C_{60}, but all even-numbered clusters of size greater than (roughly) C_{40} appeared to be almost as inert as C_{60} itself. They are far more inert than one would expect for any sort of open graphitic sheet.

This observation led to the suggestion that all these large even-numbered clusters may have tied up all their dangling bonds by taking the form of closed

202

spheroidal shells. As with C_{60} it is generally possible to construct many such closed nets of pentagonal and hexagonal rings. Figure 5 shows one possibility for C_{72}. Using Euler's theorm it is rather straightforward to prove that all such closed nets of n atoms have exactly 12 pentagons and n/2 - 10 hexagons (refs. 12, 22,23). Therefore only even-numbered clusters are capable of closing -- a fact providing a ready explanation of the measured higher reactivity of the odd-numbered carbon clusters. The smallest closed shell possibility would be C_{20} in the form of a dodecahedron (12 pentagons, 0 hexagons), although this species would almost certainly be far too strained to be stable. The saturated analog, dodecahedrane, $C_{20}H_{20}$ has almost perfect tetrahedral bond angles and is a known and quite stable molecule (ref. 44). With the exception of C_{22} all larger even-numbered clusters may assume the form of one of these geodesically rigid, closed spheroidal shells. The architectural parallel has led us to refer to these species in general as the "fullerenes" of which C_{60}, "buckminsterfullerene", is the prototypical example.

IV. SYMMETRY, STRAIN CONCENTRATION, AND THE ADJACENCY OF PENTAGONS

The number 60 is rather extraordinary. It was the base of the Babylonian number system, from which we derive the current convention of dividing hours and minutes into 60ths, and the circle into 360 degrees. Continued use of this ancient practice likely stems from the ready factorability of the number 60: it and its multiples are the most highly factorable of all integers (eg. all members of the series {1,2,3,4,5,6} are factors simultaneously only for 60 and its multiples). A related, but more important property of 60 in the current context is that it is the number of proper rotations in the largest point group, the icosahedral group, I_h. As a direct consequence, 60 is the largest number of objects that can be arranged on the surface of a sphere such that each is exactly equivalent to every other.

As a side point, it is reasonable to argue that 120 is even more special since there are actually 120 elements in the icosahedral group, and one could arrange 120 objects on a sphere with each related to every other by an element in the group (for an example see ref 12). But only 60 of these 120 symmetry elements are proper rotations, the rest either involve inversion, reflection, or improper rotations -- symmetry operations which interconvert left and right-handedness. The 120 equivalent objects then fall in two sets of 60: one left-handed, the other right-handed.

In the case of spheroidal networks of 60 vertices, there are two distinct ways of generating an icosahedral structure: the truncated icosahedron consisting of 12 pentagons and 20 hexagons, and the truncated dodecahedron, consisting of 20 triangles and 12 decagons. Although each of these is equivalently symmetrical, due to bond strain and resonance effects carbon far prefers forming 5 and 6 membered aromatic rings over any other possibility. Electronic structure calculations for these structures have been compared using simple Huckel techniques by Fowler and Woolrich (ref. 16), by and Klein, Seitz, and Schmaltz (ref. 22), and most recently with a somewhat higher level INDO procedure by

203

Shibuya and Yoshitani (ref. 33). All agree the truncated icosahedron is by far the most stable possible structure.

Given this soccerball structure for C_{60} as a starting point, one can begin to look for predictions of the relative stability of the other even-numbered C_n "fullerenes". Based on the overwhelming dominance of 5 and 6-membered aromatic carbon ring systems in nature, one expects these will be the most stable forms for all even-numbered carbon clusters. Each will assume the form of the most stable possible closed spheroidal net made up of 12 pentagons and $n/2 - 10$ hexagons such as shown in Figure 4 for the case of C_{72}.

In examining such structures it is easy to imagine why C_{60} should be uniquely unreactive. Because of the symmetry properties of the number 60, only for this cluster is the strain of closure distributed perfectly over all atoms. In all other clusters the strain tends to localize. For example the structure shown in Figure 4 clearly has concentrated the strain on the vertices of the pentagons, leaving fairly flat regions in the top and bottom hexagonal nets. This is a general phenomenon in the larger carbon clusters: strain concentrates at the pentagons. Kroto (ref. 45) has recently discussed this issue in some detail.

For clusters smaller than C_{70} there is another factor to consider in addition to strain. It is reasonable to expect that structures having two or more adjacent pentagons will be less stable than those where the pentagons are isolated by intervening hexagonal rings. In all known naturally occurring or synthetic carbon molecules there is no known example of a stable species having two fused 5-membered aromatic carbon rings. Interestingly, Scmaltz et. al. (ref. 38) have been able to show that C_{60} is the smallest fullerene which can avoid having two or more adjacent pentagons, and C_{70} is the next. The smallest cluster that can avoid having more than two pentagons adjacent turns out to be C_{50}, and the smallest that can avoid more than three adjacent is C_{32}. As can be seen in the cluster beam TOF mass spectra of Figs 1-3, clusters with 70, 60, or 50 atoms do, in fact, turn out to be specially abundant. Evidence for the special behavior of C_{32} has been found in fragmentation experiments (refs 46, 47) as will be discussed below when we consider the photophysics of the fullerenes and their observation in sooting flames (ref.48).

V. NEGATIVE CARBON CLUSTER UPS

Cluster beam TOF abundance distributions and cluster reactivity studies have therefore provided reasonably impressive evidence for the spheroidal carbon shell model of large carbon clusters. But for many observers such data can never be completely adequate as proof of a structural assignment. As is true with research in all areas of both metal and semiconductor clusters, a direct spectral probe of these carbon species would be highly valuable.

Since these clusters are produced cold in a supersonic beam, one might suspect that high-resolution laser probes of the electronic spectrum in the visible and ultraviolet would be an excellent general tool. In fact quite powerful techniques have been developed and applied to supersonic beams of small

clusters involving resonant 2-photon ionization (R2PI) with mass-selective detection. The published studies of the vanadium dimer (ref. 49), the copper trimer (ref 50), and the triangular SiC_2 cluster (ref. 51) are a few of the many excellent examples of the power of this R2PI spectral technique -- when it works. Unhappily, this R2PI technique generally does not work well for clusters containing more than a few atoms. In the larger clusters radiationless decay processes are generally far too fast to permit detection of the upper level before the electronic excitation is degraded into the vibrational quasicontinuum. In the case of C_{60} extensive R2PI probes have been carried out in our laboratory over large regions of the visible and ultraviolet spectrum without success. Electronic excitation in C_{60} simply does not last long enough to detect by the R2PI technique.

One general way of overcoming such difficulties is to go after a different type of electronic spectroscopy, one that works equally well for bulk materials as it does for atoms and small molecules. Such a procedure is UPS, ultraviolet photoelectron spectroscopy. Recently we have been able to implement such probes of supersonic cluster beams in a general way by developing a magnetically-focussed time-of-flight electron spectrometer which measures the energy spectrum of photoelectrons detached by pulse UV laser irradiation of mass-selected negative ions of the desired cluster (refs 52,53).

V.1 Small Carbon Cluster UPS
(Linear Chains and Monocyclic Rings)

The electronic and geometrical structure of small carbon clusters has been a topic of interest for molecular calculations over many years. In an early paper Pitzer and Clementi (ref. 54) used an elementary semi-empirical version of molecular orbital theory to conclude that linear chains should be the dominate form in carbon vapors. For such linear chains they found there should be a pronounced even-odd alternation in electronic structure: the even-numbered chains having open shell structures with a $^3\Sigma^-$ ground state (except for C_2 where $^3\Pi$ is lowest), and the odd-numbered chains having closed shell structures with $^1\Sigma^+$ ground state. The even numbered clusters were predicted to be somewhat more strongly bound and have considerably higher electron affinity than the neighboring odd clusters.

These calculations were refined a bit later by Strictler and Pitzer (ref 55) where the possibility of monocyclic ring structures were considered more extensively. For such rings there is also an even-odd alternation in the electronic structure, except now it is the even-numbered clusters (and particularly those with $4n+2$ carbon atoms, $n=1,2,3,...$) that are particularly strongly bound, with closed-shell singlet ground states and low electron affinities. In the early years of development of extended Huckel theory, Roald Hoffmann considered these small carbon clusters in detail (ref. 56). Generally, his results were consistent with those of Pitzer and his co-workers. His prediction was that the linear chains would be the favored form up through C_9. At C_{10} and above, however, Hoffmann predicted that monocyclic rings would be most stable.

Now we are in a position to test such theories using the new UPS cluster beam apparatus -- at least for the structures preferred by the negative cluster

205

ions. Figure 6 shows the UPS patterns for the small carbon cluster negative ions in the 2-9 atom range (ref. 57). The photoelectrons were detached here using a F_2 excimer laser which has a photon energy of 7.9 eV. Note that the original prediction of Pitzer and Clementi is perfectly well born out by these data. The arrows in each panel of the figure mark our estimate to the vertical photodetachment threshold from the negative cluster ion, approximately corrected for thermal and instrument resolution effects. This corresponds to the vertical electron affinity (EA) of the neutral cluster, evaluated at the geometrical configuration of the negative cluster ion. Note that the even-numbered clusters in the left-hand panels exhibit electron affinities starting near 3.2 eV for C_2 and increasing smoothly to nearly 4.4 eV for C_8. The odd-numbered clusters on the right-hand panels have considerably lower electron affinities, starting near 2.0 eV for C_3 and increasing smoothly to 3.6 eV for C_9. In addition, note that there is substantial gap between the first peak in the UPS pattern of the odd-numbered clusters and the next major feature, and that the relative intensity of this first peak compared to the second decreases steadily as a function of cluster size. This is the expected behavior of a species which as a neutral has a tightly-bound closed shell electronic structure with a large HOMO-LUMO gap -- just as predicted by Pitzer and Clementi for odd-numbered linear carbon chains.

Figure 7 show the UPS patterns for negative carbon clusters in the 6 through 29 atom size range. Here it is clear that an abrupt change in the simple even-odd alternation of the linear chains has occurred starting at C_{10}. Here again arrows have been placed at the estimated vertical photodetachment onset, giving a measure of the vertical electron affinity of the neutral form of each cluster. Instead of having an EA of over 4.5 eV as would be expected from extrapolation of the EA trend of the smaller even-numbered clusters, C_{10} clearly has an EA closer to 2.3 eV. Furthermore, starting with C_{10} the simple even-odd alternation in UPS patterns has been replaced by a period of 4, as emphasized by the arrangement of the spectra in the figure. Note that these periods of 4 begin at 10, 14, 18, 22, and 26 -- just the numbers expected from the predictions of extra stability of (4n+2)-membered monocyclic rings.

Close examination of these UPS patterns shows one particularly glaring anomaly: C_{11}. For this cluster there appear to be two overlapping small features where one larger peak is expected at the photodetachment threshold. Figure 8 resolves this mystery. Here it is seen that there really are two distinct types of negative C_{11} clusters. Here we have been able to selectively prepare one or the other by varying the method of generating the negative cluster beam. For the bottom panel the nozzle was run in such a way that a portion of the carbon cluster ions resulting from the original laser-induced plasma survived passage though the supersonic nozzle and subsequent expansion, much as has been done by other workers in this field who have studied negative carbon clusters (refs 58, 59). In contrast, the UPS data of the top panel was taken using cluster ions prepared by directing an excimer laser (ArF, 6.4 eV) into the throat of the supersonic nozzle just as the neutral clusters emerged. Slow electrons produced by photoionization of some of the carbon clusters effectively attach to other members of the neutral cluster distribution under these conditions, producing an intense cluster ion beam (see refs 60-63 for more details). The UPS patterns taken under these two conditions are quite different -- and different in an interesting way. The top UPS panel is in excellent agreement with the pattern one would have expected for a linear C_{11} chain, based on extrapolation from the C_9 UPS pattern and those of the smaller odd-numbered clusters. The bottom panel of Figure 8 is just what one would have expected for a monocyclic ring form of C_{11}, based on back-extrapolation

from the UPS patterns of C_{15}, C_{19}, C_{23}, and C_{27}. The cluster beam used to obtain the C_{11} UPS pattern in Figure 7 had been prepared using the excimer laser re-ionization technique, but apparently for that particular run the timing and laser intensity was such that an approximately 1:1 mixture of the two forms of C_{11}^- was produced.

This linear chain / monocyclic ring transition in the UPS patterns is particularly graphic in the electron affinity plot shown in Figure 9, where the EA values for each cluster were taken from the UPS data of Figures 6 and 7 at the positions of the arrows. Note that there are two points plotted for C_{11}.

The notion that carbon clusters in this size range may take the form of monocyclic rings is hardly new. The 4-fold periodicity seen in the early mass spectroscopy of carbon vapors from spark discharges (ref. 64) was used to reach this conclusion very early on in the history of carbon cluster research (refs 54,56). Recently, quite high level *ab initio* calculations have concluded that cyclic structures may be preferred for very small even-numbered clusters, eg. a rhombus for C_4 (ref. 65), and a slightly distorted hexagon for C_6 (ref 66). The UPS data shown here in Figs 6-8, and particularly the smooth EA trends, seems quite conclusive that the negative carbon clusters with <10 atoms prefer the linear chain geometry. Of course, it is likely that there is a minimum in the potential surface corresponding to a cyclic structure, and this minimum for some clusters such as C_4 and C_6 may be lowest for the <u>neutral</u> charge state of the cluster. These new UPS data only probe the favored geometry of the negative cluster ions.

For positively charged small carbon clusters there has been recently a very impressive determination that C_3^+ is a monocyclic ring (a triangle) by measurement of the "coulomb explosion" this cluster undergoes as its electrons are stripped by passage at high velocity through a target foil (ref. 67). Photodissociation cross-section measurements (ref. 68) and reactivity measurements in an FT-ICR apparatus (ref 69-71) indicate that C_{10}^+ behaves as a monocyclic ring.

The initial impetus for carbon cluster work at Rice was the question of whether the long carbon chain species so abundant in the interstellar medium could be produced effectively in condensing carbon vapors. Reaction studies performed with various reagents mixed in the helium carrier gas prior to laser generation of the carbon plasma provided a clear demonstration that long linear carbon chains can indeed be produced in this way (refs 72, 73). However, in light these new UPS results and the uniform results of quantum chemical calculations, it is now clear that carbon clusters substantially longer than 9 atoms will take the form of linear chains only in reactive conditions where the ends can be terminated by such groups as -H or -CN.

<div align="center">

V.2   Intermediate Size Carbon Cluster UPS
(Open Polycyclic Nets and Highly-Strained Cages)

</div>

Above the high twenties there is a region in the carbon cluster distribution extending up to near C_{40} that is quite difficult to study. The clusters in this intermediate region appear to be far more reactive that either the small or large

carbon clusters, so that unusually when one samples carbon clusters from a vapor-phase distribution the concentration of these active species is abnormally low. This effect can be seen in the TOF cluster mass spectrum shown in Figure 2. It was first pointed out by Rohlfing, Cox, and Kaldor in their original supersonic carbon cluster study (ref 5). These intermediate range clusters are difficult to generate, and thus far we have been unable to obtain repeatable, dependable UPS data for them. In order to generate useable cluster beams in this mass region, the cluster source must be run such that growth reactions in the nozzle are abruptly terminated, and there is little opportunity for the most stable form of a particular cluster to dominated the population. As a result, the cluster beam always appears to contain a mixture of closed- and open-shell species, and the resultant UPS patterns are ill-defined.

We suspect it is in this 28-40 atom cluster size range that the switch in cluster growth occurs from 2-dimensional monocyclic rings to polycyclic (quasi-graphitic) nets, to growing 3-dimensional spirals and highly strained cages.

<center>

V.3   Large Carbon Cluster UPS
(C_{60} and the Fullerenes)

</center>

As shown in the bimodal distribution that generally characterizes carbon cluster distributions from these high pressure supersonic nozzle sources, above C_{40} cluster abundance grows again, and there is a dramatic even-odd alternation in the cluster reactivities and intensities. Figure 10 shows the UPS patterns obtained for selected even-numbered clusters in the 48-84 atom size range (ref. 63). The odd-numbered clusters throughout this region display only broad, featureless UPS pattern characteristic of open-shell species. As is evident from the figure, the even-numbered clusters in this region generally do not have highly structured UPS patterns either. However, there are a few clear exceptions to this rule of little structure: C_{50}, C_{60}, and C_{70}. Note that of all the clusters in this 48-84 region, C_{60} has the lowest photodetachment onset (therefore the lowest EA) and the clearest initial peak, with the broadest gap to the next feature. This low electron affinity and substantial gap in the UPS pattern is indicative of a tightly bound, electronically closed shell molecule.

The UPS data of Figure 10 were taken with an ArF excimer laser (6.4 eV photon energy) used to produce the photoelectrons. Recently, we have begun re-examining these clusters with the new, higher photon energy F_2 excimer laser. Qualitatively the results are unchanged, except that now the difference between C_{60} and the other clusters is far more pronounced. Figure 11 shows the most recent picture of the UPS pattern for C_{60}^- taken with the F_2 laser at 7.9 eV. Sufficient structure is now resolved that detailed comparison with electronic structure calculations begins to be reasonable.

As mentioned earlier, C_{60} has been the subject of many calculations over the past few years (refs 11-40). One interesting result emerging from these calculations is that the molecular orbitals near the top of the valence band of this cluster are almost purely made up of radially directed 2p atomic orbitals with a small amount of 2s hybridization on each of the 60 carbon atoms. The result is that even simple Huckel MO treatments which neglect the tangentially-directed orbitals will be fairly good approximations near the HOMO-LUMO region of the cluster. This point was first clearly made by Newton and Stanton based on

<center>208</center>

MNDO calculations (ref. 24), and independently confirmed by LMTO studies of Satpathy (ref. 25), the PRDDO work of Marynick and Estreicher (ref. 28), the DV-Xalpha calculations of Hale (ref. 27), and the CNDO/S method of Larsson, Volosov, and Rosen (ref. 35). A portion of the high-lying molecular orbital energy levels predicted by a simple Huckel calculation of icosahedral C_{60} is shown on the right hand side of Figure 11.

For the neutral C_{60} cluster the HOMO is (as shown in Fig. 11) an orbital of h_u symmetry; it is filled with 10 electrons, giving a closed-shell electronic ground state of ^1A_g symmetry. The C_{60}^- negative ion ground state is then produced by adding one electron to the next highest orbital, the t_{1u} symmetry level marked in the figure as the LUMO of the neutral molecule, producing a state of overall $^2T_{1u}$ symmetry. The first peak in the UPS spectrum for such a molecule would then arise from the photodetachment of the lone electron in the t_{1u} orbital. The binding energy of this orbital (approximately the vertical electron affinity) has been estimated to be 2.4 eV in the recent CNDO/S calculations of Rosen and coworkers (ref. 35). As seen in the UPS data of the figure, this is in fairly good agreement with measured value of roughly 2.8 eV.

The next lowest level, the h_u orbital that is the HOMO of the neutral cluster, is estimated in this same CNDO/S calculation to have a binding energy of 7.55 eV -- also in excellent agreement with the measured ionization potential of C_{60} which is known to lie in the range between 6.4 and 7.9 eV (refs. 43, 74). From the fact that the F_2 laser is able to directly photoionize weakly-bound van der Waals adducts of C_{60} without fragmentation (ref. 75), we suspect the IP threshold is quite sharp, and located only slightly below the 7.9 eV photon energy of this laser. The agreement with the calculated 7.55 eV IP value of Rosen et. al. is therefore quite impressive.

Since the t_{1u} LUMO is calculated at 2.4 eV binding energy and seen in the UPS at roughly 2.8 eV, one might expect the next feature in the UPS spectrum would arise from removal of electrons from the h_{1u} HOMO level and appear near the calculated 7.5 eV binding energy for this orbital. However, there is a detail here: these are 1-electron molecular orbitals, and the energy levels calculated by simply adding the orbital energies of all electrons corresponds to the energy of a single Slater determinant (single configuration) multielectron wavefunction for C_{60}. While the electronic ground states of C_{60}, C_{60}^+, and C_{60}^- will be fairly well approximated by these single-determinant wavefunctions, the excited electronic states of C_{60} will not. IP and EA estimates from the HOMO and LUMO binding energy calculations should therefore be fairly accurate, but calculations of the excited electronic states of C_{60} must consider configuration interaction. This is true for simple aromatic molecules like benzene and naphthalene, it will certainly be true here for C_{60}.

In the absence of configuration interaction, predicted UPS pattern for C_{60}^- would show a peak due to removal of electrons from the h_u HOMO orbital shifted 7.5-2.4 = 5.1 eV higher in binding energy than the first peak arising from removal of the t_{1u} LUMO electron. Since there are 10 electrons in the h_u orbital, this second feature in the UPS spectrum should be roughly ten times more intense than the first (assuming, as is the case here, that the same type of atomic orbitals are involved in each molecular orbital). Removal of an electron from the h_u orbital of C_{60}^- gives rise to 8 excited electronic states with a configuration of $(h_u)^9(t_{1u})^1$: $^{1,3}T_{1g}$, $^{1,3}T_{2g}$, $^{1,3}G_g$, and $^{1,3}H_g$. Since these states are all of different symmetries, they will not mix through configuration interaction. But at

higher energy there are many excited states of these same symmetries arising from other orbital configurations (for example: $(h_g)^9(t_{1g})^1$). The result of configuration interaction will then be to mix in these higher configurations, pushing the excited electronic states with $(h_u)^9(t_{1u})^1$ parentage down in energy. As a consequence what would have been a sharp single peak in the UPS spectrum associated with removal of 1 of the 10 electrons in the h_u HOMO will now appear as an extensively broadened photodetachment band at considerably lower binding energy. Although a definite assignment must await comparison to a detailed calculation, the broad band appearing in the UPS data between 4 and 5 eV binding energy is a reasonable candidate. In fact the integrated area under this band does turn out to be roughly ten times larger that the first band at 2.8 eV.

The UPS data shows there is another, more intense band of excited states in the region of 6.5 to 5.5 eV. Referring to the predicted molecular orbital pattern, it is reasonable to tentatively assign this band to the states over overall ungerade symmetry arising from generation of a hole in the nearly degenerate g_g and h_g orbitals. Here the integrated intensity is about %80 of that expected for the 18 electron occupancy of these orbitals. Intensity in the UPS data then drops off sharply in the 6-7 eV region, as would be expected from the calculated molecular orbital pattern: the next available orbital (g_u) is far deeper.

In summary, the new UPS data make it clear that the electronic structure of C_{60} is much like that expected of the soccerball geometry. As expected for such a well-bound closed shell molecule, the electron affinity is low -- much lower than any other carbon cluster in this size range, and quantitatively in agreement with the best calculations. In addition, the C_{60}^- UPS pattern is far more highly structured than any other carbon cluster in the region. For such a huge, highly unsaturated molecule it is hard to imagine such a simple UPS pattern arising from anything but the sort of rigid, highly symmetrical structure proposed. In addition, the details of this pattern appear consistent with theoretical expectations.

Of course the assignments of the excited state structure in the C_{60}^- UPS data postulated above can only be considered tentative at this point. Larsson, Volosov, and Rosen have calculated the excited electronic states of C_{60} allowing for interaction between 250 configurations of lowest energy (ref. 35). Such calculations can provide the sort of information needed for a detailed comparison with the new UPS data.

VI.   PHOTOPHYSICS OF THE POSITIVE CARBON CLUSTER IONS

Regardless of the ultimate answer to the question of the structure of C_{60}, it is by far the most stable small cluster of carbon. As such it may be made in abundance wherever carbon condenses. From the standpoint of astrophysics, one of the most significant aspects of this molecule is its photophysics: how much excitation can C_{60} withstand? How efficient is C_{60} at re-radiating excitation energy? What are its photofragmentation products? Since in most astrophysical environments of interest carbon is ionized, these questions on the photophysics of C_{60} are particularly relevant for the positive ion, C_{60}^+. And, of course, it would be nice to know how the answers to these questions compare with those for all other clusters of carbon.

Using tandem time-of-flight techniques (ref. 76) a good deal of progress has been made in understanding the photophysics of mass-selected carbon cluster positive ions over the past several years. For the small positive cluster ions (up to C_{20}^+) Geusic and co-workers at Bell Labs (ref. 68) found that laser excitation in the visible or ultraviolet resulted in only a single fragmentation pathway: successive loss of C_3. This was true both of even-numbered and odd-numbered clusters. More recently we have reproduced and extended these studies to larger clusters (ref. 46). Two distinct photophysical regimes were found. The first applies to all positive carbon clusters of 31 atoms or less. As found by the Bell Labs group for the smaller members of this set, all these clusters photodissociate exclusively by the loss of a neutral C_3 fragment. Dominance of this fragmentation channel over that for the loss of C or C_2 is easy to rationalize since C_3 is far more stable. For the reasons first put forward by Pitzer and Clementi (ref. 54) the even-numbered small carbon clusters such as C_2 are not as strongly bound as is C_3. The cohesive energy of the diatomic C_2, for example is only 3.1 eV/atom, while that of C_3 is 4.2 eV/atom (see ref. 77 for the most recent estimate of small carbon cluster binding energies). Raghavachari and Binkley have recently considered the photofragmentation of these small carbon clusters in detail. They concluded that the C_3 loss channel is energetically preferred for all carbon clusters at least up to C_{10}^+ -- even when one considers the possibility that some of the even clusters may be monocyclic rings (ref. 77). The uniform observation of C_3 loss from the small carbon clusters is therefor unsurprising.

The second distinct photophysical regime for positive carbon clusters applies to the most stable (unreactive) forms of all clusters larger than 33 atoms. The qualifier here about the most stable forms is necessary since many valence isomers of these larger carbon clusters are possible, and the presence of the more reactive, less well-bound versions is sometimes detected in the supersonic beams (see ref. 46 for details). For the most stable forms of the even-numbered clusters in this >33 cluster size range the photophysics is again simple, but is also quite surprising: these even "fullerenes" are extremely difficult to photodissociate, and when at sufficiently high laser excitation they do ultimately fragment, they do so by the loss of C_2. For example, Figure 12 shows the result of a tandem-TOF photodissociation experiment on C_{60}^+ irradiated by a 2 mj cm^{-2} pulse of ArF excimer laser radiation (6.4 eV). As is evident in the figure, C_{58}^+ is the primary photoproduct. As the laser fluence is increased the smaller even numbered fullerenes are produced by successive C_2 loss.

Figure 13 shows the photodissociation laser fluence dependence on the observed primary (C_{58}^+) and secondary (C_{56}^+) protoproduct from C_{60}^+ mass-selected in the tandem-TOF apparatus and irradiated with a single 10 nsec pulse of ArF radiation (1930 Å, 6.4 eV) with a fluence per pulse which was varied under computer control and measured for each shot (ref. 46). Note that there is a minimum fluence below which no significant fragment signal is seen, and that this critical minimum fluence is greater for the C_{56}^+ photoproduct. This proves that dissociation of C_{60}^+ is a multiphoton process at this wavelength, and that C_{56}^+ is a secondary photoproduct.

It is difficult in such experiments to obtain an accurate measure of the photon order of a dissociation process once this order is greater than one. Inhomogeneities in the laser beam profile, imperfect overlap between laser beam

and target beam, and temporal irregularities in the laser pulse all have the effect of making the apparent photon order seem much lower than it really is (see the appendix of ref. 76 for a numerical example). In addition, the C_{60}^+ supersonic cluster ion source used for these experiments is now known not to have cooled the internal degrees of freedom of the carbon clusters completely. It is possible the species studied had internal temperatures in excess of 400K. Given the predicted vibrational frequencies of C_{60} (refs. 34,39), one can calculate that a 400K vibrational temperature means the average cluster starts off the photodissociation experiment with 3.7 eV internal energy even before the first photon is absorbed.

By careful fitting of photofragmentation fluence measurements such as that shown in Figure 12, we are confident that the C_{60}^+ --> C_{58}^+ + C_2 primary fragmentation event is at least a 3 photon process at 1930 Å. Because of the photon order measurement difficulties mentioned above, it is likely that the real photon order for C_{60}^+ fragmentation is even higher. The main point here is that C_{60}^+ is an extremely photoresistant molecule, requiring more than 12.8 eV to dissociate, and probably much more. In fact it is the most photoresistant positive cluster ion we have ever encountered in such an experiment, including such extremely tightly bound clusters as Ta_{10}^+.

Similar photodissociation experiments to those shown in Figure 12 have been carried out for a wide range of the large even carbon cluster "fullerenes". All behave essentially the same way: they are all highly resistant to fragmentation, and when they do, they do so by the loss of C_2. As the photodissociation laser fluence is increased, the successive C_2 loss process generates successively smaller even numbered cluster ion products. But, as shown in Figure 14, this C_2 loss process does not go on forever. The C_2 loss continues down until C_{32}^+ is formed. At this point, instead of loosing C_2 to become C_{30}^+, this critical cluster virtually explodes in to small pieces, most of which are smaller than C_{20}^+.

As discussed a bit earlier, C_2 is a very strange fragment to find coming out of any large cluster of carbon; C_3 or virtually any other larger fragment would be energetically far more favorable. After extensive consideration over the past year in our laboratory and others, only one mechanism has been advanced which can successfully explain this C_2 loss. It involves the concerted removal of C_2 from a closed fullerene net. As the top panel of Figure 15 shows, it is possible to extract a C_2 unit from such a closed net while at the same time beginning to form the next smaller fullerene whenever two pentagons are adjacent in the net. This mechanism has the advantage that it readily explains why the sequential photodissociation process senses that C_{70}^+, C_{60}^+ , and C_{50}^+ are particularly stable as high order grand-daughters (ref. 46). As shown in the lower two panels of Fig. 15, concerted mechanisms for loss of longer even-numbered chains are available for the fullerenes as well. Dissociation by these longer chain pathways appears to be necessary in order to explain certain observations in the long-term decay of intensely irradiated fullerenes (see ref. 46 for details). Such processes may be a significant source of the long carbon chain species in the interstellar medium.

The only alternatives to the closed fullerene net model for these clusters would have to involve either interlinked polyacetylene chains or open graphitic sheets. From the measurements on the <32 atom clusters which we know are linear chains and monocyclic rings, all these species fragment readily at low laser

212

fluence, and they do so by the very sensible path of C_3 loss. For any open graphitic net it is easy to see that C_3 loss from one of the edges is always available, and involves no more bond breakage or rearrangement than would C_2 loss. Since C_3 removal is by far the lowest energy channel, there is no reason to expect C_2 loss to occur.

On the other hand, a closed, <u>edgeless</u> carbon network such as that postulated for the fullerenes has a far more difficult time producing any fragments. This, we believe, is why the photophysics of these species is so difficult to activate, and why the C_2 loss channel suddenly becomes important. Incidentally, this model also naturally explains why the C_2 loss terminates abruptly at C_{32}^+ and why this last cluster dissociates explosively. Each C_2 loss from a fullerene produces the next smaller fullerene. Schmaltz et. al. have shown (ref. 38) that the total out-of-plane angle strain necessary to close a graphitic sheet into a fullerene shell is to first order independent of the size of the cluster. As the cluster gets smaller, the strain per carbon atom increases, until at some point the fullerene shell will be too unstable to survive. Apparently the smallest viable fullerene shell is C_{32}.

VI.1 The Semifullerenes

The only remaining well-defined carbon cluster species to be discussed are the large odd-numbered species, C_n^+, where n is an odd number > 33. The photophysics of these is quite simple. The primary photoprocess is loss of a single C atom, or in some cases loss of a single C_3. After this initial loss the resultant even-numbered daughter ion will (if sufficiently excited) begin loosing C_2 pieces just as if it had begun as a member of the even-numbered fullerene family. The fact that the high-order grand-daughters in this successive C_2 loss process appear to sense the special nature of the "magic" fullerene numbers (70,60,50) indicates that these grand-daughters are, in fact, fullerenes themselves (see ref. 46 for details). Since it is impossible to generate a closed fullerene net with an odd number of carbon atoms, they must originally be open. But the fact that the primary photoprocess is often loss of a single C atom strongly suggests that these species are nearly as close to closure into a fullerene net as they can get -- hence the name "semifullerene".

Very similar results have been obtained by Bowers and coworkers by examining the fragmentation routes of metastable carbon cluster ions produced by laser vaporization of a graphite target in a vacuum (ref. 47) although their explanation of these fragmentation pathways is completely different.

VII. PHOTOPHYSICS OF METAL-CONTAINING FULLERENES

There is one other class of photophysical experiments that have recently provided further indication that the fullerenes are in fact closed, hollow shells. Shortly after our first realization that C_{60} may have the form of a hollow sphere, we published evidence that a single metal atom could be trapped inside (ref. 41). The key experimental result was that shown in Figure 16. This shows the TOF mass spectrum of large clusters in a supersonic beam made by laser-vaporization of a graphite disc which had been impregnated with $LaCl_3$. There are two mass spectra show here, both obtained using an ArF excimer laser to photoionize the species in

213

the beam. The bottom panel shows the spectrum obtained at very low probe laser fluence (<0.01 mJ cm^{-2}) such that multiphoton excitation and fragmentation of the clusters was minimized as much as possible. As seen in the figure, the TOF mass spectrum obtained in this way was highly complicated, containing features due to bare carbon clusters and clusters containing one La atom which each peak broadened to the high mass side and the whole spectrum riding on a broad, unresolved baseline. In a TOF mass spectrometer such asymmetrically broadened peaks and underlying baseline signal are a signature of extensive fragmentation of the parent ions during the initial acceleration process in the sample region of the spectrometer. In fact the baseline signal was considerably worse than shown here; most has been cut out in the figure in order to get the partially resolved peaks on the same scale as the top panel.

This top panel, on the other hand, was taken at a much higher ArF excimer laser fluence (1-2 mJ cm^{-2}). Previous experience with ordinary organometallic complexes in this group (refs 78,79) had led us to expect that even strongly bound complexes would be readily fragmented at these laser fluence, resulting in a complete loss of ligands, leaving only the charged (often multiply charged) bare metal atom or metal oxide. As a group organometallic complexes are not particularly photoresistant. So it is quite impressive to see in the top panel of Figure 15 that large organometallic clusters survive high laser excitation. Not only do they survive, but (aside from C_{60}^+ and C_{70}^+) species of the form C_nLa^+ are the only ions detected in this mass range. Furthermore, there is no evidence of clusters surviving with more than one La atom, suggesting that there is only one strong binding site. Similar results were obtained with Ca, Sr, and Ba when the corresponding chloride was incorporated in the graphite disc.

Kaldor and co-workers have cautioned that due to photoionization artifacts this early evidence that the clusters have only a single strong metal atom binding site may be misleading (ref. 74). They have shown that in some cases such as potassium, carbon clusters with 2 or 3 metal atoms can be detected in the supersonic beam (refs. 80, 81). However, their own experiments show that only C_nK^+, the clusters with a single metal atom, are sufficiently stable to survive at high laser fluences (ref. 81).

One test of the hypothesis that the metal atom in these complexes is trapped inside a closed fullerene shell is to examine the photophysics. If the M in the C_nM^+ complexes is completely surrounded by an edgeless carbon net, then such complexes should be at least as photoresistant and the bare C_n^+ clusters, and when they fragment they should do so by the loss of C_2, leaving the metal atom still trapped inside a now somewhat smaller fullerene shell. As shown in Figure 17, this is exactly what happens.

Here the $C_{60}La^+$ and C_{72}^+ clusters were extracted from a supersonic beam and injected into an ion cyclotron resonance apparatus (refs. 82, 83). The ions are trapped in a high vacuum in the analysis cell of this apparatus by the combination of a strong (6 Tesla) axial magnetic field and an electrostatic barrier. After exposure to roughly 10^4 thermalizing collisions with a neon buffer gas to cool the translational and internal degrees of freedom of the clusters to near the 120K wall temperature of the trap, these clusters were subjected to 50 shots of an ArF laser at roughly 4 mJ cm^{-2} fluence per shot. Detection of the contents of the analysis cell was accomplished by coherent RF excitation of the cyclotron motion of the ions, followed by amplification and digitization of the oscillating image charge currents in the side electrodes of the cell. The Fourier transform of this

time-dependent signal then provides a sensitive, non-destructive measure of the contents of the cell at extremely high mass resolution. This technique, known as Fourier transform ion cyclotron resonance (FT-ICR) is one of the most promising new probes for cluster ions.

As is evident from comparison of the top panel where no laser excitation was used, the result of such intense laser irradiation has been to fragment a portion of both the original types of clusters in the cell. As expected, both show exactly the same photophysical pathway: successive loss of C_2. Also as expected, the metal-containing cluster is a bit more photoresistant than the bare fullerene (although part of this extra stability is due in this case to the fact that a $C_{60}M^+$ cluster is being compared to one of the less stable fullerenes, C_{72}^+).

These experiments have been extended to a wide variety of the C_nLa^+ / C_{n+12}^+ metal complex / bare cluster pairs with similar results. FT-ICR photolysis experiments have also been done with C_nK^+ clusters. They too are extremely photoresistant, and ultimately fragment by the C_2 loss route. One particularly intriguing result is that the C_2 loss process for C_nK^+ breaks off abruptly at $C_{44}K^+$. Just as C_{32}^+ is the last fullerene seen in the high order photofragmentation of the bare carbon clusters, $C_{44}K^+$ appears to be the smallest viable potassium-containing carbon cluster.

Computer modeling of the C_nK^+ clusters reveals a very simple explanation for this break off at 44. The ionic radius of K^+ is 1.33 Å. Assuming a 1.45 Å carbon-carbon bond length and a 1.6 Å carbon van der Waals radius, these modeling tests show that there is plenty of room for the electronically closed shell K^+ atom to fit inside the closed C_n fullerene net as long as $n>44$. For $C_{44}K^+$ a few bonds need to be lengthened to roughly 1.5 Å to permit the K^+ atom to fit. But for C_{42} smaller fullerenes the amount of bond stretching required becomes quite prohibitive. Experiments are currently in progress to see if this critical C_nM^+ cluster size scales correctly with the size of the alkali ion.

VIII. STATISTICAL FRAGMENTATION & RADIATIVE COOLING

In the course of these FT-ICR photolysis experiments an observation was made that is particularly relevant to the question of survival of these carbon cluster ions in the interstellar medium. The fluence dependence of the fragmentation process shown in Figure 17 was the same as that found in the tandem TOF experiments (Fig. 13) where only a single laser shot could be used prior to monitoring the fragments. In the ICR apparatus the carbon cluster ions can be exposed to many laser pulses over an extended time period (over 30 seconds) while the background pressure is so low ($< 10^{-8}$ torr) that the only de-excitation pathway is radiative. Under these conditions when the fluence per 10 nsec pulse of the ArF laser was less than 0.5 mJ cm^{-2}, no fragmentation whatever was seen from C_{60}^+ -- even when the repetition rate of the laser pulses was raised to 50 Hz and the clusters were irradiated for over 30 seconds.

From measurements to be described below in the section on optical spectroscopy of fullerenes, we know that the absorption cross-section of C_{60}^+ at the 1930 Å wavelength of the ArF laser is roughly 5×10^{-16} cm^2. At a fluence of 0.5 mJ cm^{-2} the probability of a 1-photon excitation event in any particular C_{60}^+ cluster is then roughly %20. Without radiative cooling the typical C_{60}^+ cluster

would then receive 0.2 x 1500 = 300 ArF laser photons of excitation. The fact that no dissociation was observed indicates that C_{60}^+ is very efficient in radiating away excitation energy on a millisecond timescale.

Given the absence of and C--H oscillators in this molecule, it is initially rather surprising that radiative cooling is so efficient. But here the key feature is that the molecule is so large (174 vibrational modes) that for a statistical dissociation process with even a moderate activation barrier, an extreme amount of superexcitation is required to produce fragmentation on a relevant time scale. If C_{60}^+ has the icosahedral structure we have suggested, any UV photoexcitation will initially be globally distributed over the cluster. Since electronic radiationless energy decay is fast in C_{60} (otherwise R2PI would work), it will certainly have to dissociate starting from a statistical distribution of the available energy among the 174 vibrational modes. This is a nearly macroscopic bath of vibrational states. For example, given the recent estimates for the vibrational frequencies of C_{60} (ref. 34,39), one can readily calculate that even at only 1.0 eV vibrational energy in the cluster there are over 6×10^{18} vibrational states per cm^{-1}.

If one accepts the closed carbon net structure for the fullerenes, it is easy to find on energetic grounds alone that the dissociation barrier of C_{60}^+ to form $C_{58}^+ + C_2$ will be at least 4 eV (reference to Figure 15 shows that 2 carbon-carbon bonds are lost in this process, each worth over 2 eV). In addition, the concerted loss process of Fig. 15 is orbitally-forbidden in the Woodward-Hoffmann sense (ref. 84), and should therefore have a substantial activation barrier. So it is difficult to imagine the barrier to C_2 loss from C_{60}^+ being less than something like 5 eV. Even with optimistic assumptions as to the nature of the activated process, a crude RRKM calculation of the unimolecular fragmentation rate of C_{60}^+ shows that the average cluster would require over 26 eV excitation energy in order to dissociate over such a barrier in less than 0.1 second.

While radiative cooling should be very slow for moderate levels of excitation, 26 eV is not moderate -- it is equivalent to the average thermal excitation of C_{60}^+ at 1800K. Approximated simply as a black body, the radiative cooling rate of C_{60}^+ would be extremely fast at these levels of excitation. However, C_{60}^+ will not act as a black body at these temperatures, even though the high excitation will certainly speed the radiative cooling rate considerably. The lowest excited electronic state of C_{60}^+ capable of emitting electric dipole radiation is likely to be above 1 eV, and there will be little weight for such excited electronic states in the typical quasicontinuum wavefunction even at 26 eV. Vibrational excitation of the ground electronic state will dominate, with an average of 2-3 quanta in each of the 174 vibrational modes. Excited C_{60}^+ will therefore be a poor black body emitter. The bulk of the radiation from the superheated molecule should still be expected to be emitted in the infrared at frequencies near each of the four ir-active t_{1u} modes (calculated frequencies: 1628, 1353, 718, and 577 cm^{-1} -- see refs. 34, 39). The highest two of these have been calculated to have large dipole moment derivitives (3.1 and 2.0 debye $Å^{-1}$, respectively for the 1628, and 1353 cm^{-1} modes) and should therefore be particularly effective IR emitters (ref. 39). This fact coupled with the high degree of vibrational excitation make the result of millisecond (or faster) radiative cooling times seem reasonable, although it would be interesting to see a detailed calculation.

216

Regardless of the explanation for the efficient radiative cooling, the clear experimental result is that excitation energy sufficient to fragment C_{60}^+ must be pumped in within considerably less than 20 milliseconds in order to be effective. In low flux astrophysical environments where the highest energy photon is insufficient to fragment C_{60}^+ in a single step, this molecule should therefore be quite stable. Because of its unique symmetry, its size, and the perfect absence of edges providing easy, low energy fragmentation pathways, C_{60}^+ may be the most photoresistant of all possible molecules. Because of its ability to cool by infrared emission, it may be able to survive unshielded in the interstellar medium for very long periods of time.

Interestingly, there appears to be a close agreement between the calculated frequency of the two most intense IR active modes in C_{60} and two of the more intense interstellar IR emissions in the 6 to 8 micron region (see, for example, ref. 85).

IX. OPTICAL SPECTROSCOPY

Direct optical probes of C_{60} and similar large clusters have proved difficult. Due to the low densities of the cluster species in the supersonic beam and the need to distinguish the spectrum of one cluster from all others, direct absorption methods are generally not applicable. The principal techniques of obtaining electronic spectra of clusters in supersonic beams rely either on resonant photoionization (R2PI) or fluoresence detection, both of which effectively require the excited electronic states of the cluster to live for a nanosecond or more. Neither C_{60}, nor any of the other clusters of carbon beyond C_3 seem to have such long-lived excited states -- at least none have been found in the extensive surveys carried out thus far.

IX.1 Neutral C_{60}

In spite of these difficulties, one moderately successful spectral experiment has recently been reported for C_{60} using a van der Waals probe technique (ref. 75). Here C_{60} was cooled in a supersonic helium jet which had been seeded with a few percent concentration of a small closed shell molecule -- benzene, for example. By arranging for a particularly intense expansion, some of the C_{60} molecules were cooled sufficiently that a benzene molecule became attached to the surface, held only by weak van der Waals bonds. In the subsequent supersonic beam the concentration of this C_{60}-benzene complex was detected by direct 1-photon ionization with a F_2 excimer laser at 1570 Å (7.9 eV), followed by TOF mass spectrometric detection of the C_{60}^+-benzene ion. One of the virtues of this approach is that one is guaranteed to be dealing with an extremely cold molecule. Based on other known van der Waals complexes, the C_{60}-benzene van der Waals bond is unlikely to be stronger than 1500 cm^{-1}. Vibrational predissociation of such van der Waals complexes generally proceeds readily on a microsecond timescale, so that only those C_{60}-benzene complexes with less than 1500 cm-1 internal energy are likely to last the 700 microsecond flight time from the source in this beam apparatus to the detection chamber. In the case of C60-benzene, this implies the effective vibrational temperature of the complex in the beam must be less than 30 K.

Since the C_{60}-benzene van der Waals complex is so weakly bound, its spectrum may be probed simply by passing a tuneable laser down the axis of the molecular beam. The result of absorption of a laser photon is inevitably dissociation of the van der Waals complex, and this fact may be sensed as a depletion of the van der Waals complex concentration in the beam. Such depletion spectroscopies are notoriously insensitive since they try to detect a small change in a large, erratic signal. Nonetheless, it was successful in this case. Figure 17 shows a single, isolated absorption feature detected by this van der Waals probe technique. It is roughly 50 cm-1 wide, located near 3860Å, and rides on an underlying absorption continuum. The estimated absorption cross-section at the peak is 1-2×10^{-17} cm2, while that of the underlying continuum is 2-4 times smaller. The top spectrum was recorded for the C_{60}-benzene complex, the bottom for the methylene chloride complex, C_{60}-CH_2Cl_2. The fact that this absorption feature appears only slightly shifted in both complexes, and the fact that neither benzene nor methylene chloride have absorptions anywhere close to this wavelength proves that this isolated absorption band is due to the cold C_{60} molecule. Since the shift is so slight when such a drastic change is made in the type of van der Waals probe molecule, one expects the corresponding absorption feature in the bare C_{60} molecule will be close to this same wavelength.

The assignment of this 3860 Å band of C_{60} is not yet certain. Based on its position (3.22 eV) and the fact that it appears alone, it has been tentatively assigned as the 0-0 band of the first electric dipole allowed electronic transition of icosahedral C_{60} ($^1T_{1u} \leftarrow\; ^1A_g$). The calculations of Rosen and coworkers predict this transition should be found at 3.6 eV, and have an oscillator strength of 0.08. The fact that the observed transition has an oscillator strength of only 0.004 gives reason to suspect the assignment may be in error (see ref. 75). Due to difficulties in laser technology and apparatus time, the spectral search was completed only over the regions 3350 -- 3450Å, 3650 -- 4000 Å, 4350 -- 4450 Å, and 5750 -- 5900 Å. Although the 3860 Å band was the only spectral feature observed in these regions, given the rather poor sensitivity of the technique other weaker transitions might have been missed. It is quite possible that the real $^1T_{1u} \leftarrow\; ^1A_g$ origin lies in one of the as yet unscaned regions. Regardless of the final assignment of the 3860 Å band, it is impressive that such a relatively narrow, isolated absorption feature exists in a carbon cluster this large.

Perhaps more interesting is where this C_{60} molecule does not absorb: it is nearly transparent in the visible. Even with a 200 mJ cm^{-2} laser pulse, the 5320 Å green output of a doubled Nd:YAG laser produced no noticeable fragmentation of the C_{60}-benzene van der Waals complex. The absorption cross-section of C_{60} at this wavelength is less than 2×10^{-19} cm^2. Furthermore, careful spectral scans in the regions of the strongest known diffuse interstellar bands (4428, 5780, 5797 Å -- ref. 86) showed conclusively that neutral C_{60} is not responsible.

IX.2 Optical Spectroscopy of C_{60}^+

The positive ion of C_{60} is likely to be the most abundant form in the interstellar medium. Unlike the closed-shell icosahedral neutral molecule where the first dipole-allowed transition is not expected until the ultraviolet, the open-shell C_{60}^+ is expected to have 10 - 15 allowed electronic origins sprinkled throughout the visible spectrum. Given the rigidity of the icosahedral net, and the small change in net bonding produced by promotion of 1 out of 239 bonding

valence electrons, these 10-15 electronic bands are expected to be confined mostly to just the 0-0 vibrational origins, with small splittings due to Jahn-Teller effects. In other words, C_{60}^+ is an outstanding candidate for the carrier of the diffuse interstellar lines (refs. 7, 86).

An attempt has been made to record the spectrum of C_{60}^+ by an extension of the way the neutral molecule was done: using a van der Waals probe. However, the interaction between benzene and C_{60}^+ is considerably stronger than between benzene and neutral C_{60}. This becomes vastly more of a problem in the excited electronic states of the complex since configuration interaction with the C_{60}-benzene$^+$ charge transfer states is strong. The C_{60}^+-CH_2Cl_2 complex should be somewhat better in this regard, but we have found the spectrum of both complexes to be structureless. Either there are no sharp spectral features for C_{60}^+, or the benzene and methylene chloride probes cause too much of perturbation. Efforts are underway to use a more innocent probe such as neon, although this will require a major change in cluster source technology.

Although the benzene and methylene chloride probes have not provided any sharp spectral features, they have permitted estimates of the absorption intensity over broad wavelength regions. As with the neutral C_{60}, the cold positive ion is effectively transparent in the visible (cross section $< 2 \times 10^{-19}$ cm^2). In the ultraviolet, preliminary absorption cross-section estimates were roughly the same as those measured for the neutral: 2×10^{-16} cm^2 at 248 nm, 7×10^{-16} cm^2 at 1930 Å. Considering the significant possibility that C_{60}^+ or some of the other fullerenes may be responsible for the interstellar UV extinction feature (ref. 87), these absorption cross-section measurements should be extended and performed with care. Again, it would be best to complete these only after the technology is in hand to study less perturbed complexes such as C_{60}^+-neon.

X. ASTROPHYSICAL C_{60}

Granting the fact that C_{60} is so special and so readily produced in the laser-produced carbon vapor of these supersonic nozzles, it is still by no means obvious that it should be generated in significant quantities in any astrophysical environment. When considering why such spheroidal nets should form spontaneously, my colleagues and I proposed a mechanism in which a growing graphitic sheet incorporates pentagons on its periphery so as to minimize the dangling bonds (ref. 43). For each new pentagon included, a few new carbon-carbon bonds could be made from what were previously dangling bonds on the hexagonal lattice. Each added pentagon causes further curling of the growing sheet, but the instability associated with adjacent pentagons tends to keep them isolated from each other by an intervening hexagon. The result is a propensity for a graphite sheet to curl with a curvature that is exactly that of C_{60}. Once the growth has gone far enough that the opposite edges approach, there is a possibility that the spheroidal net will close, thereby producing a fullerene. However, most such growing imperfect nets would be expected to overlap the opposite edge, burying it inside, and continuing to grow in spiralling shells around a central core. Figure 19 shows an idealized image of such a growing spiral particle. Sumio Iijima has reported evidence for such spiralling carbon particles visualized in an electron microscope (see ref. 88 and references therein).

While this is a topologically appealing mechanism, it depends for its driving force on the presence of dangling bonds on the periphery of the growing

nets.   In the more relevant environment of a sooting flame -- or the outer atmosphere of a carbon-rich red giant -- there is plenty of hydrogen around to tie up these dangling bonds.   Why would there be any tendency to curl then?   We suspect the answer is the same as it is to the question of why carbon nets grow at all under these conditions: at these high temperatures carbon-carbon bonds are preferred over carbon-hydrogen bonds.   At high temperatures in hydrocarbon systems, carbon is most stable as graphite; hydrogen is most stable as H_2.

Regardless of the reasons advanced pro and con for the likelihood of C_{60} formation in sooting environments, there has now been a direct measurement of its presence in high abundance along with the other fullerenes in acetylene-oxygen and benzene-oxygen flames (ref. 48).   If C_{60} is formed in these sooting flames, it is almost certainly formed in abundance also in carbon-rich red giants, since the temperatures and compositions are quite similar.   Given the unique photophysical stability of C_{60}^+, it appears possible that this molecule may be able to survive migration far away from its original star.   It may therefore be both very abundant and very important in the interstellar medium.

The list of possible astrophysical implications of abundant circumstellar and interstellar C_{60}, the fullerenes in general, and the spiral graphitic objects of the sort shown in Fig. 19, is long and (by now) widely known.   Given sufficient funding and sustained interest, the combination of laboratory experiments of the sort described here and the new generation of space-based spectral probes may be able to settle most (if not all) of these conjectures within the next decade.

REFERENCES

1. Dietz, Thomas G; Duncan, Michael A.; Powers, David E; and Smalley, Richard E.: Laser Production of Supersonic Metal Cluster Beams.   J. Chem. Phys., vol. 74, 1981, pp 6511-6512.

2. Powers, David E; Hansen, Steven G.;   et. al.: Supersonic Metal Cluster Beams: Laser Photoionization Studies of Cu_2. J. Phys. Chem., vol. 86, 1982, pp 2556-2560.

3. Hopkins, John B; Langridge-Smith, Patrick R. R.; Morse, Michael D., and Smalley, Richard E.: Supersonic Metal Cluster Beams of Refractory Metals: Spectral Investigations of Ultracold Mo_2.

4. O'Brien, Sean C.; Liu, Yuan; et. al.: Supersonic III-V Semiconductor Cluster Beams: Ga_xAs_y. J. Chem. Phys., vol. 84, 1986, pp 4074-4079.

5. Rohlfing, Eric A.; Cox, Donald M.; and Kaldor, Andrew: Production and Characterization of Supersonic Carbon Cluster Beams.   J. Chem. Phys., vol 81, 1984, pp 3322-3330.

6. Heimann, R. B.; Kleiman, J.; and Salansky, N. M.: A Unified Structural Approach to Linear Carbon Polytypes, Nature, vol 306, 1983, pp 164-167.

7. Kroto, Harry W.; Heath, James R.; O'Brien, Sean C.; Curl, Robert F., and Smalley, Richard E.: C_{60}: Buckminsterfullerene. Nature, vol. 318, 1985, 162-163.

8. Osawa, Eiji: Superaromaticity, Kagaku, vol.25, 1970, pp 854-855.

9. Bochvar, D. A.; and Gal'pern, E. G.: Hypothetical Systems: Carbondecahedron, s-Icosahedrane, and Carbon-s-icosahedron.Dokl. Akad. Nauk. SSSR vol. 209, 1973, pp 239-241.

10. Davidson, R. A.: Theoret. Chim. Acta, vol. 58, 1981, pp 193-195.

11. Stanlevich, I. V.; Nikerov, M. V.; and Bochvar, D. A.: The Structural Chemistry of Crystalline Carbon: Geometry, Stability, and Electronic Spectrum. Russian Chem. Rev., vol. 53, 1984, pp 640-655.

12. Haymet, Anthony D. J.: C_{120} and C_{60} Archimedean Solids Constructed from sp^2 Hybridized Carbon Atoms, Chem. Phys. Lett., vol. 122, 1985, pp 421-424.

13. Haymet, Anthony D. J.: Footballene: A Theoretical Prediction for the Stable, Truncated Icosahedral Molecule C_{60}. J. Am. Chem. Soc., vol. 108, 1986, pp 319-321.

14. Haddon, R. C.; Brus, Louis E.; and Ragavachari, Krishnan: Electronic Structure and Bonding in Icosahedral C_{60}, Chem. Phys. Lett., vol. 125, 1986, pp 459-464.

15. Disch Raymond L. and Schulman, Jerome M.: On Symmetrical Clusters of Carbon Atoms: C_{60}, Chem. Phys. Lett., vol. 125, 1986, pp 455-456.

16. Fowler, P. W.; and Woolrich, J.: Pi-Systems in Three Dimensions. Chem. Phys. Lett., vol. 127, 1986, pp 78-83.

17. Ozaki, Masa-aki; and Takahashi, Akira: On Electronic States and Bond Lengths of the Truncated Icosahedral C_{60} Molecule, Chem. Phys. Lett., vol. 127, 1986, pp 242-244.

18. Stone, A. J. and Wales, D. J.: Theoretical Studies of Icosahedral C_{60} and Some Related Species, Chem. Phys. Lett., vol. 128, 1986, pp 501-503.

19. Fowler, P. W.: How Unusual is C_{60}? Magic Numbers for Carbon Clusters, Chem. Phys. Lett., vol. 131, 1986, pp 444-450.

20. Hess, Jr., B. Andres; and Schaad, L. J.: The Stability of Footballene. J. Org. Chem., vol. 51, 1986, 3902-3903.

21. Klein, Douglas J.; Schmalz, Thomas G.; Hite, G, E.; and Seitz, William A.: Resonance in Buckminsterfulleren. J. Am. Chem. Soc., vol. 108, 1986, pp 1301-1302.

22. Klein, D. J.; Seitz, W. A., and Schmalz, T. G.: Icosahedral Symmetry Carbon Cage Molecules. Nature, vol. 323, 1986, pp 703-706.

23. Schmaltz, Thomas G.; Seitz, William A.; Klein, Douglas J; and Hite, George E.: C_{60} Carbon Cages, Chem. Phys. Lett., vol. 130, 1986, pp 203-207.

24. Newton, Marshall D. and Stanton, Richard E.: Stability of Buckminsterfullerene and Related Carbon Cluster, J. Am. Chem. Soc.,vol. 108, 1986, pp 2469-2470.

25. Satpathy, Sashi: Electronic Structure of the Truncated-Icosahedral C_{60} Cluster, Chem. Phys. Lett., vol. 130, 1986, pp 545-550.

26. Haddon, R. C.; Brus, L. E.; Raghavachari, Krishnan: Rehybridization and PI-Orbital Alignment: The Key to the Existence of Spheroidal Carbon Clusters. Chem. Phys. Lett., vol. 131, 1986, pp. 165-169.

27. Hale, Paul D.: Dicrete-Variational-Xalpha Electronic Structure Studies of the Spherical C_{60} Cluster: Prediction of Ionization Potential and Electronic Transition Energy, J. Am. Chem. Soc., vol. 108, 1986, pp 6087-6088.

28. Marynick, Dennis S. and Estreicher, Stephen: Localized Molecular Orbitals and Electronic Structure of Buckminsterfullerene, Chem. Phys. Lett., vol. 132, 1986, pp 383-386.

29. Harter, William G.; and Weeks, David E.: Rovibrational Spectral Fine Structure of Icosahedral Molecules, Chem. Phys. Lett., vol. 132, 1986, pp 387-392.

30. Kataoka, Masahiro; and Nakajima,Takeshi: Geometrical Structures and Spectra of Carannulene and Icosahedral C_{60}. Tetrahedron, vol. 42, 1986, pp 6437-6442.

31. Luthi, Hans Peter; and Almlof, Jan: Ab Initio Studies on the Thermodynamic Stability of the Icosahedral C_{60} Molecule "Buckminsterfullerene", Chem. Phys. Lett., vol. 135, 1986, pp 357-360.

32. Laszlo, I.; and Udvardi, L.: On the Geometrical Structure and UV Spectrum of the Truncated Icosahedral Sixty-Atom Carbon (C_{60}) Molecule. Chem. Phys. Lett., vol. 136, 1987, pp 418-422.

33. Shibuya, Tai-Ichi; and Yoshitani, Masaaki: Two Icosahedral Structures for the C_{60} Cluster, Chem. Phys. Lett., vol. 137, 1987, pp 13-16.

34. Wu, Z. C.; Jelski, Daniel A.; and George, Thomas F.: Vibrational Motions of Buckminsterfullerene, Chem. Phys. Lett., vol 137, 1987, pp 291-294.

35. Larsson, Sven; Volosov, Andrey; and Rosen, Arne: Optical Spectrum of the Icosahedral C60 -- "Follene-60", Chem. Phys. Lett., vol. 137, 1987, pp. 501-503.

36. Elser, V.; and Haddon, R. C.: Icosahedral C_{60}: An Aromatic Molecule with a Vanishingly Small Ring Current Magnetic Susceptibility. Nature, vol. 325, 1987, pp. 792-794.

37. Schulman, Jerome M.; Disch, Raymond L.; Miller, Mitchell A.; and Peck, Rosalie C.: Symmetrical Clusters of Carbon Atoms: The C24 and C60 Molecules, Chem. Phys. Lett., vol. 141, 1987, pp 45-48.

38. Schmaltz, Thomas G.; Seitz, William A.; Klein, Douglas J.; and Hite, G. E.: "Elemental Carbon Cages", J. Am. Chem. Soc., vol. 110, 1988, (in press).

39. Stanton, Richard E.; and Newton, Marshall D.: Normal Vibrational Modes of Buckminsterfullerene. J. Phys. Chem., vol. 92, (to be published).

40. Hayden, G. W.; and Mele, E. J.: The Pi Bonding in the Icosahedral Carbon (C_{60}) Cluster. Phys. Rev. B: Condens. Matter., vol. 36, 1987, pp 5010-5015.

41. Heath, J. R.; O'Brien, S. C.; et. al.: Lanthanum Complexes with Spheroidal Carbon Shells. J. Am. Chem. Soc., vol. 107, 1985, pp. 7779-7780.

42. Morse, M. D.; Geusic, M. E; Heath, J. R.; and Smalley, R. E.: Surface Reactions of Metal Clusters II: Reactivity Surveys with D_2, N_2, and CO. J. Chem. Phys., vol. 83, 1985, pp 2293-2304.

43. Zhang, Qing-Ling, O'Brien, S. C.; et. al.: The Reactivity of Large Carbon Clusters: Spheroidal Carbon Shells and Their Possible Relevance to the Formation and Morphology of Soot. J. Phys. Chem., vol. 90, 1986, pp 525-528.

44. Paquette, Leo. A.; Ternansky, R. J.; Balogh, D. W.; and Kentgen, G.: J. Am. Chem. Soc., vol. 105, 1983, pp 5446-.

45. Kroto, H. W.: The Stability of the Fullerenes Cn (n - 28, 32, 36, 50, 60 and 70), Nature, vol. 329, 1987, pp 529-531.

46. O'Brien, S. C.; Heath, J. R.; Curl, R. F.; and Smalley, R. E.: Photophysics of Buckminsterfullerene and other Carbon Cluster Ions, J. Chem. Phys., vol. 88, 1988, (in press).

47. Radi, Peter P.; Bunn, Thomas L.; Kemper, Paul R.; Molchan, Michele E.; and Bowers, Michael T.: A New Method for Studying Carbon Clsters in the Gas Phase: Observation of Size Specific Neutral Fragment Loss from Metastable Reactions of Ma Selected Cn+, n<-60, J. Phys. Chem. vol. 30, 1988, (in press).

48. Gerhardt, Ph.; Loffler, S.; and Homann, K. H.: Polyhedral Carbon Ion in Hydrocarbon Flames, Chem. Phys. Lett., vol. 137, 1987, pp 306-310.

49. Langridge-Smith, Patrick R. R.; Morse, M. D.; Hansen, G. P.; Smalley, R. E., and Merer, Anthony J.: The Bond Length and Electronic Structure of V_2. J. Chem. Phys., vol. 80, 1984, pp 593-600.

50. Morse, M. D.; Hopkins, J. B.; Langridge-Smith, P. R. R.; and Smalley, R. E.: Spectroscopic Studies of the Jet-Cooled Copper Trimer. J. Chem. Phys., vol. 79, 1983, pp 5316-5328.

51. Michalopoulos, D. L.; Geusic, M. E.; Langridge-Smith, P. R. R.; and Smalley, R. E.: Visible Spectroscopy of Jet-Cooled SiC_2: Geometry and Electronic Structure.

52. Cheshnovsky, O.; Yang, S.; Pettiette, C. L.; Craycraft, M. J.; Liu, Y.; and Smalley, R. E.: Ultraviolet Photoelectron Spectroscopy of Semiconductor Clusters: Silicon and Germanium. Chem. Phys. Lett., vol. 138, 1987, pp. 119-124.

53. Cheshnovsky, O.; Yang, S.; Pettiette, C. L.; Craycraft, M. J.; and Smalley, R. E.: Magnetic Time-of-Flight Photoelectron Spectrometer for Mass-Selected Negative Cluster Ions. Rev. Sci. Instrum., vol. 58, pp. 2131-2137.

54. Pitzer, K. S.; and Clementi, E.: Large Molecules in Carbon Vapor, J. Am. Chem. Soc., vol. 81, 1959, pp 4477-4485.

55. Strickler, S. J.; and Pitzer, K. S.: Energy Calculations for Polyatomic Carbon Molecules. in Molecular Orbitals in Chemistry, Physics, and Biology ed. by P. O. Lowdin and B. Pullman (Academic Press, New York, 1964), pp 281-291.

56. Hoffmann, Roald: Extended Huckel Theory -- V: Cumulenes, Polyenes, Polyacetylenes and C_n. Tetrahedron, vol. 22, 1966, pp 521-538.

57. Yang, S.; Taylor, K. R.; et. al.: UPS of 2-30 Atom Carbon Clusters. Chem. Phys. Lett., (to be published).

58. Bloomfield, Louis; Geusic, Michael E.; Freeman, Richard R.; and Brown, W. L.: Negative and Positive Cluster Ions of Carbon and Silicon. Chem. Phys. Lett., vol. 121, 1985, pp 33-37.

59. Hahn, M. Y.; Honea, E. C.; Paguia, A. J.; Schriver, K. E.; Camerena, A.M.; and Whetten, Robert L.: Magic Numbers in C_n^+ and C_n^- Abundance Distributions. Chem. Phys. Lett., vol. 130, 1986, pp 12-16.

60. O'Brien, Sean C.; Heath, James R.; Kroto, Harry W.; Curl, Robert F.; and Smalley, Richard E.: A Reply to "Magic Numbers in C_n^+ and C_n^- Abundance Distributions" Based on Experimental Observations. Chem. Phys. Lett., vol. 132, 1986, pp 99-102.

61. Zheng, L-S.; Brucat, P. J.; Pettiette, C. L.; Yang, S. and Smalley, R. E.: Formation and Photodetachment of Cold Metal Cluster Negative Ions. J. Chem. Phys., vol. 83, 1985, pp. 4273-4274.

62. Liu, Yuan; O'Brien, Sean C.; et. al.: Negative Carbon Cluster Ion Beams: New Evidence for the Special Nature of C_{60}. Chem. Phys. Lett., vol. 126, 1986, pp 215-217.

63. Yang, S.; Pettiette, C. L.; et. al.: UPS of Buckminsterfullerene and Other Large Clusters of Carbon. Chem. Phys. Lett., vol. 139, 1987, pp. 233-238.

64. Hintenberger, H.; and Dornenburg, E.: Das Auftreten Vielatomiger Kohlenstoffmolekule in Hochfrequenzfunken Zwischen Graphitelectroden. Z. Naturforsch., vol. 14a, 1959, pp 765-767.

65. Magers, David H.; Harrison, Robert J.; and Bartlett, Rodney, J.: Isomers and Excitation Energies of C_4. J. Chem. Phys., vol. 84, 1986, pp 3284-3290.

66. Ragavachari, Krishnan; Whiteside, R. A.; and Pople, John A.: Structure of Small Carbon Clusters: Cyclic Ground State of C_6. J. Chem. Phys., vol. 85, 1986, pp 6623-6628.

67. Faibis, A.; Kanter, E. P.; Tack, L. L.; Bakke, E.; and Zabransky, B. J.: Geometry and Structure of C_3^+. J. Phys. Chem., vol. 91, 1987, pp 6445-6447.

68. Geusic, M. E.; Jarrold, M. E.; McIlrath, T. J.; Freeman, R. R.; and Brown, W. L.: Photodissociation of Carbon Cluster Cations. J. Chem. Phys., vol. 86, 1986, 3862-3869.

69. O'Keefe, A. O.; Ross, M. M.; and Baronovski, A. P.: Production of Large Carbon Cluster Ions by Laser Vaporization. Chem. Phys. Lett., vol. 130, 1986, 17-19.

70. McElvany, S. W.; Creasy, W. R.; and O'Keefe, A. O.: Ion-Molecule Reaction Studies of Mass-Selected Carbon Cluster Ions Formed by Laser Vaporization. J. Chem. Phys., vol 85, 1986, pp. 632-633.

71. McElvany, Stephen, Nelson, H. H.; Baronovski, Andrew P.; Watson, Clifford H.; and Eyler, John R.: FTMS Studies of Mass-Selected Large Cluster Ions Produced by Direct Laser Vaporization.

72. Heath, J., R.; Zhang, Q.; et. al.: The Formation of Long Carbon Chain Molecules during Laser Vaporization of Graphite. J. Am. Chem. Soc., vol. 109, 1987, pp. 359-363.

73. Kroto, H. W.; Heath, J. R.; et. al.: Long Carbon Chain Molecules in Circumstellar Shells. Ap. J., vol. 314, 1987, pp. 352-355.

74. Cox, Donald M.; Trevor, Dennis J.; Reichmann, Kenneth C.; Kaldor, Andrew: $C_{60}La$: A Deflated Soccerball?. J. Am. Chem. Soc., vol. 108, 1986, pp 2457-2458.

75. Heath, James R.; Curl, Robert F.; and Smalley, Richard E.: The UV Absorption Spectrum of C_{60} (Buckminsterfullerene): A Narrow Band at 3860 Å. J. Chem. Phys., vol. 87, 1987, pp. 4236-4238.

76. Brucat, Phillip J.; Zheng, Lan-Sun; Pettiette, Claire L.; Yang, Shihe, and Smalley, Richard E.: Metal Cluster Ion Photo-fragmentation. J. Chem. Phys., vol. 84, 1986, pp 3078-3088.

77. Raghavachari, Krishnan; and Brinkley, J. S.: Structure, Stability, and Fragmentation of Small Carbon Clusters. J. Chem. Phys., vol. 87, 1987, pp. 2191-2197.

78. Duncan, Michael A.; Dietz, Thomas G.; and Smalley, Richard E.: Laser Synthesis of Metal Clusters from Metal Carbonyl Microcrystals. J. Am. Chem. Soc., vol. 103, 1981, pp. 5245-5246.

79. Dietz, Thomas G.; Duncan, Michael A; et. al.: Spectral Narrowing and Infrared Laser Fragmentation of Jet-Cooled $UO_2(hfaa)_2TMP$ and $UO_2(hfaa)_2THF$: Volitile Uranyl Compounds. J. Chem. Phys., vol. 77, 1982, pp. 4417-4426.

80. Kaldor, A.; Cox, D. M.; Trevor, D. J.; and Zakin, M. R.: The Chemistry and Physics of Molecular Surfaces. Z. Physik D., vol. 3, 1986, pp. 195-204.

81. Cox, D. M.; Reichmann, K. C.; and Kaldor, A.: Carbon Clusters Revisited: Comments on the "Special" Behavior of C_{60} and Other Large Carbon Clusters. J. Chem. Phys., vol. 88, 1988, (to be published).

82. Elkind, J. L.; Alford, J. M.; Weiss, F. D.; Laaksonnen, R. T.; and Smalley, R. E.: FT-ICR Probes of Silicon Cluster Chemistry. J. Chem. Phys., vol. 87, 1987, pp 2397-2398.

83. Elkind, J. L.; Weiss, F. D.; Alford, J. M.; Laaksonnen, R. T.; and Smalley, R. E.: FT-ICR Studies of H_2 Chemisorption on Niobium Cluster Cations. J. Chem. Phys., (to be published).

84. Woodward, R. B.; and Hoffmann, R: <u>The Conservation of Orbital Symmetry</u> (Verlag Chemie Academic Press, Weinheim, 1971).

85. Allamandola, L. J.; Sandford, S. A.; and Wopenda, B.: Interstellar Polycyclic Aromatic Hydrocarbons and Carbon in Interplanetary Dust Particles and Meteorites. Science, vol. 237, 1987, no. 4810, pp. 56-59.

86. Herbig, G. H.; and Soderblom, R. R.: ... Astrophys. J., vol. 252, 1982, pp 610- .

87. Rabilizirov, R.: The Role of Cavities and Mantles in the Ultraviolet Extinction Peak of Graphite spheres with Particular Reference to a Possibly Discovered C_{60} Structure. Astrophys. Space Sci., vol. 125, 1986, pp 331-339.

88. Iijima, Sumio: The 60-Carbon Cluster has been Revealed!. J. Phys. Chem., vol. 91, 1987, pp 3466-3469.

VAPORIZATION
LASER

IO ATM
HELIUM

INTEGRATION
CUP

ROTATING GRAPHITE
DISC
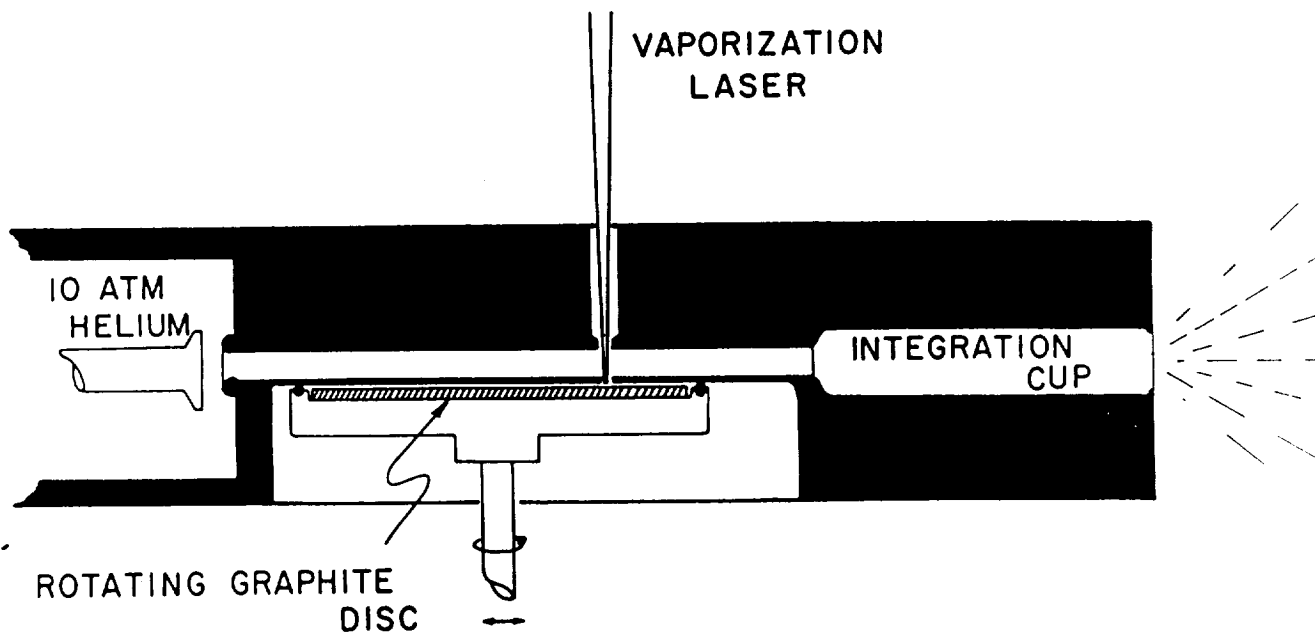
Figure 1.– Schematic of pulsed laser vaporization nozzle source for production of supersonic beams of carbon clusters.

CARBON ATOMS PER CLUSTER
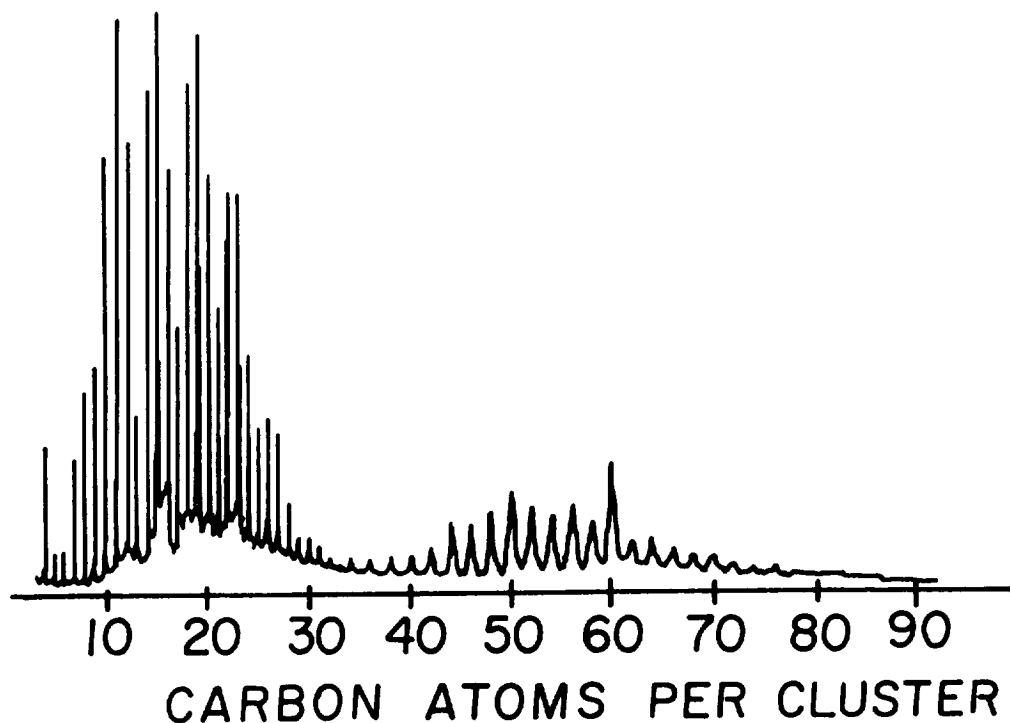
Figure 2.– Time of Flight (TOF) mass spectrum of carbon clusters prepared in a supersonic beam by laser vaporization of a graphite disc in the nozzle device of the type shown in Fig. 1. Ionization of the neutral clusters was done by photoionization with an ArF excimer laser beam (1930 Å, 6.4 eV).
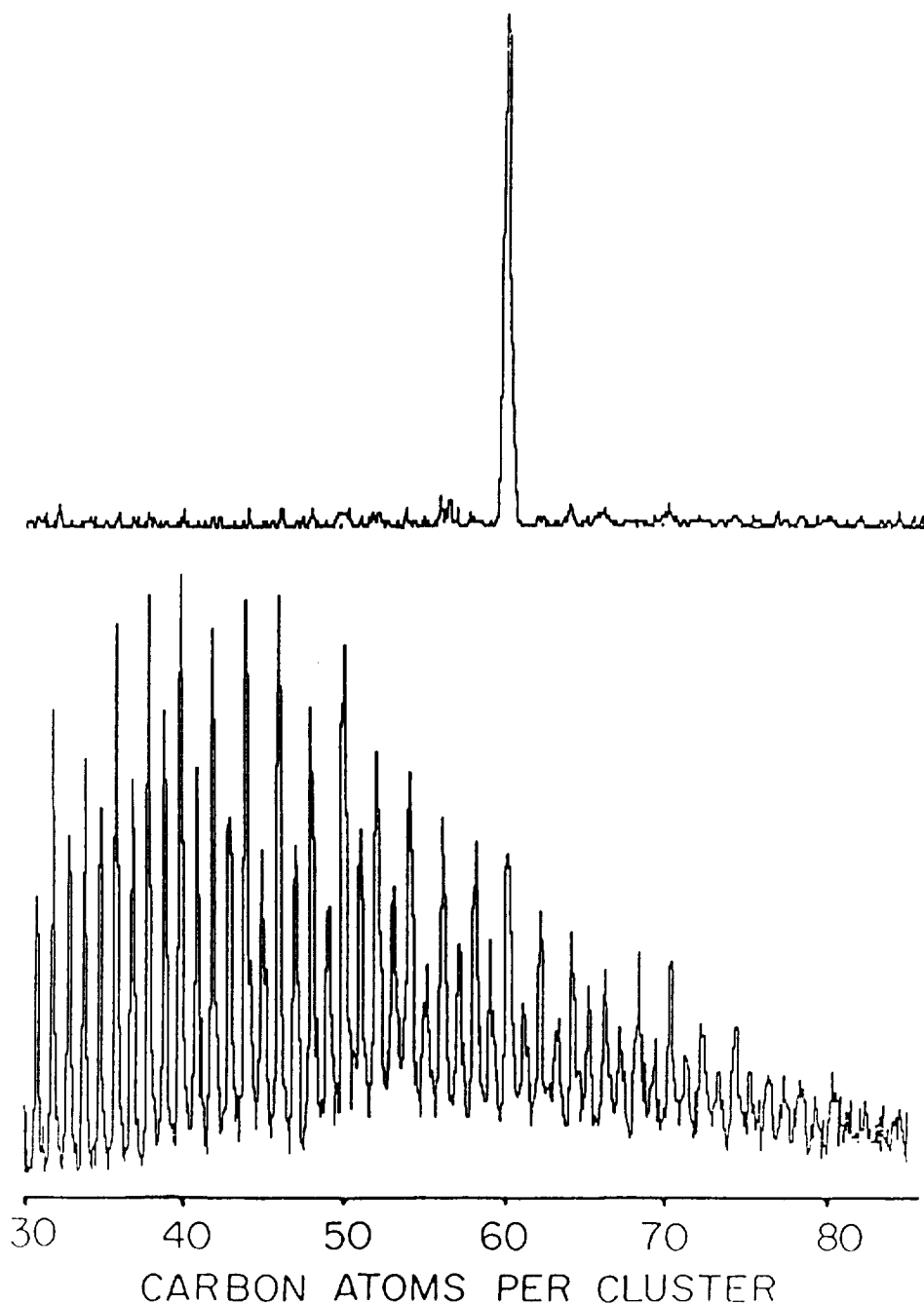
Figure 3.– Time of flight mass spectrum of carbon clusters in a supersonic beam when the nozzle source was operated under minimal clustering/reaction conditions (bottom panel), and maximum clustering/reaction conditions (top panel). Ionization was accomplished by direct one-photon photoionization with a F_2 excimer laser (1570 Å, 7.9 eV). Note that only C_{60} survives. It has not grown in intensity, rather the other clusters have dropped in intensity due to cluster growth reactions in the nozzle.

control

60 sccm   NO

10   20   30   40   50   60   70
CARBON ATOMS PER CLUSTER
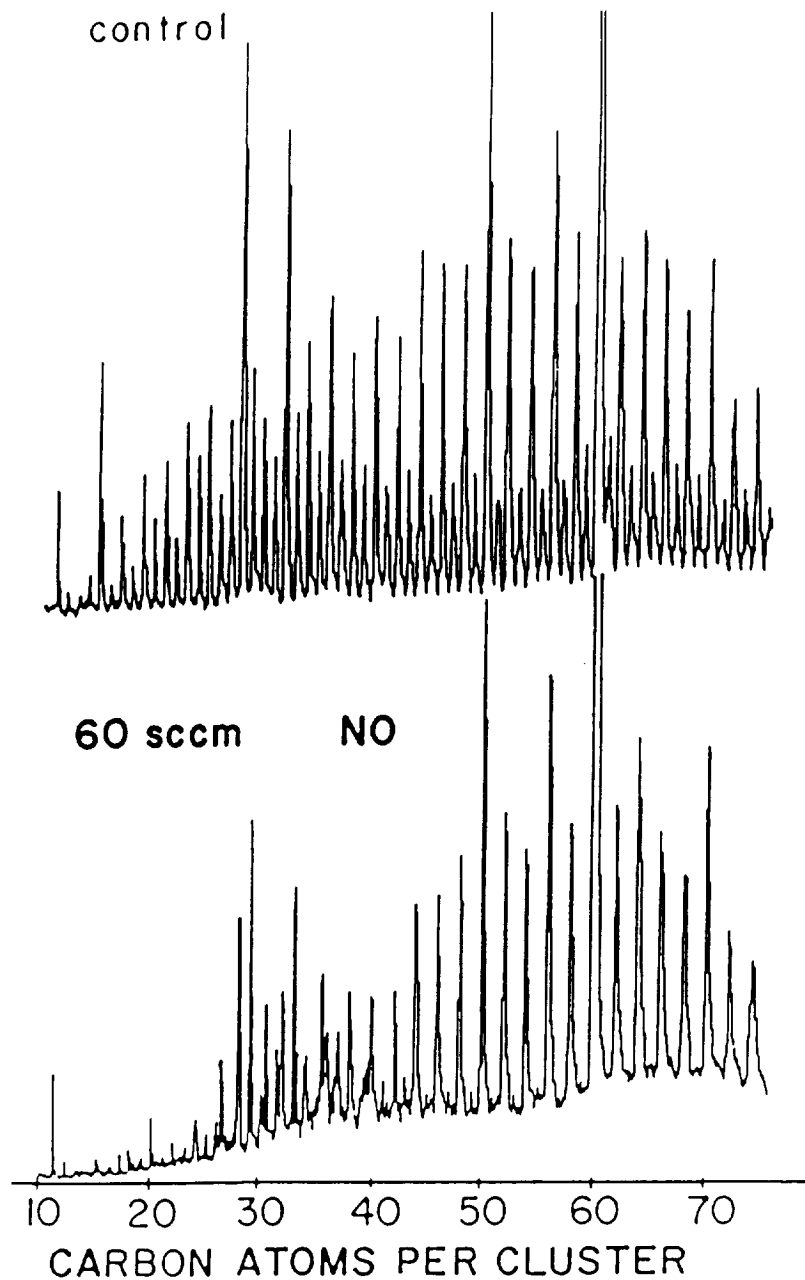
Figure 4.– Reactivity study with NO on carbon clusters. The top panel shows the cluster distribution prior to injection of the reactant (an F_2 excimer laser was used for ionization). The bottom panel shows this distribution after 170 microseconds of exposure to NO in a helium buffer gas at near room temperature in a fast flow reactor.
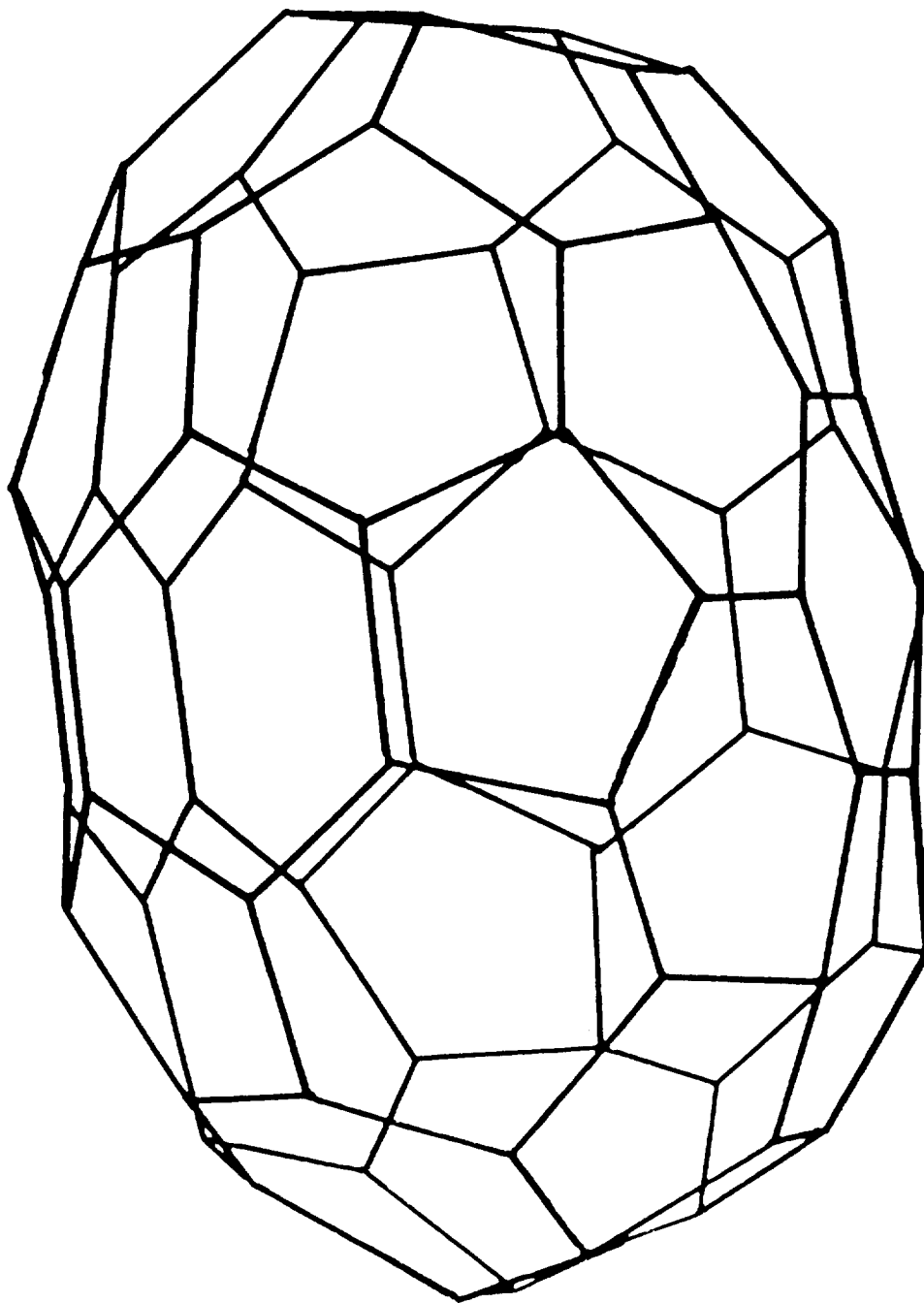
Figure 5.– One possible closed spheroidal network structure for the C_{72} fullerene. All fullerene structures are closed nets containing 12 pentagons and n/2-10 hexagons. Note the concentration of strain at the pentagons. These sites are suspected to be the most reactive. Due to its perfect symmetry, C_{60} is the only fullerene with perfectly distributed (and therefore minimized) strain.

230
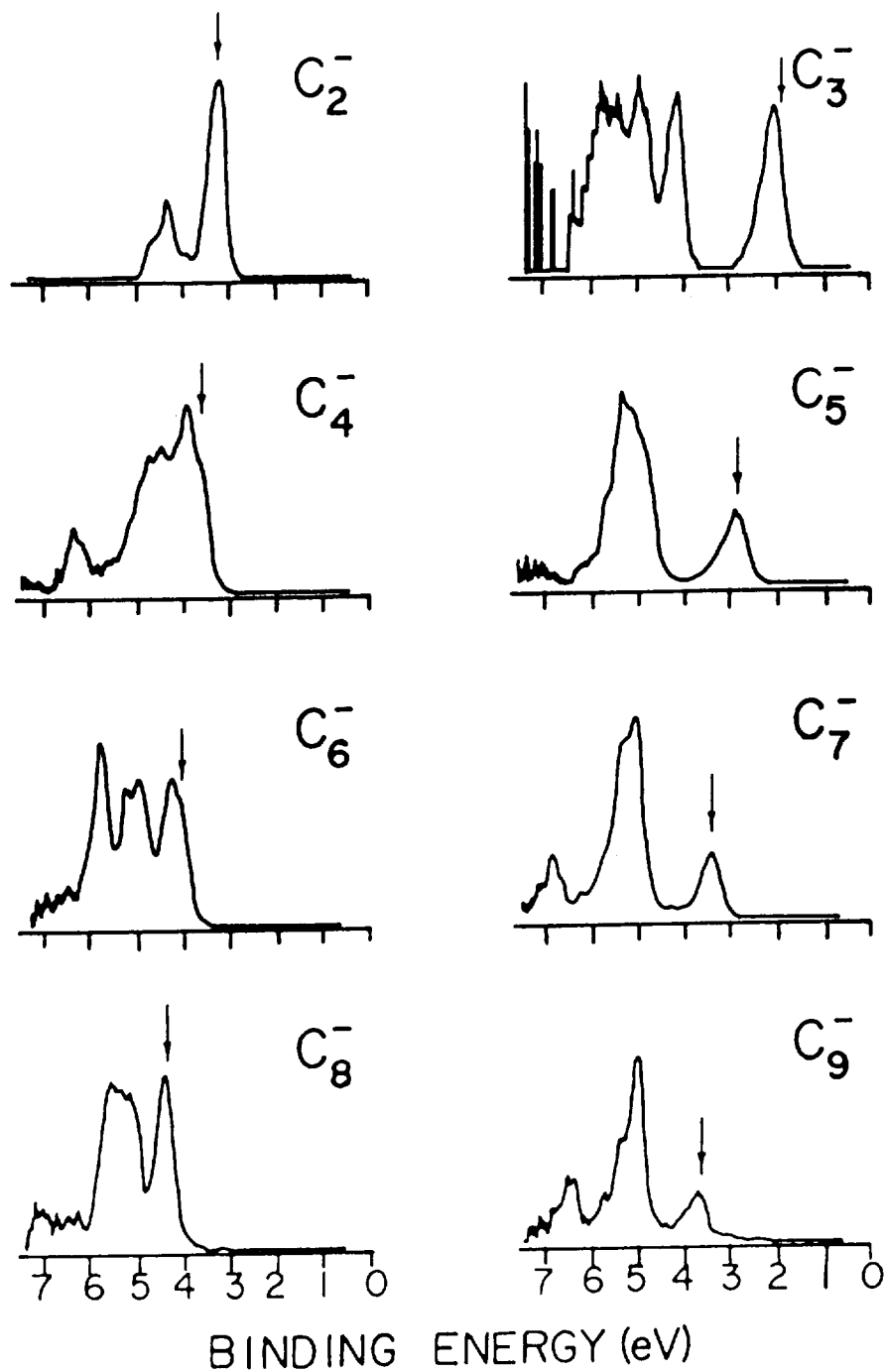
Figure 6.– Ultraviolet Photoelectron Spectrum (UPS) of C_n^- in the n=2 to 9 region. An F_2 excimer laser (7.9 eV) was used for photodetachment of the appropriate mass-selected negative cluster ion. The arrow in each panel is an estimate of the vertical photodetachment threshold energy roughly corrected for thermal effects and instrument resolution.

ELECTRON   BINDING   ENERGY (eV)
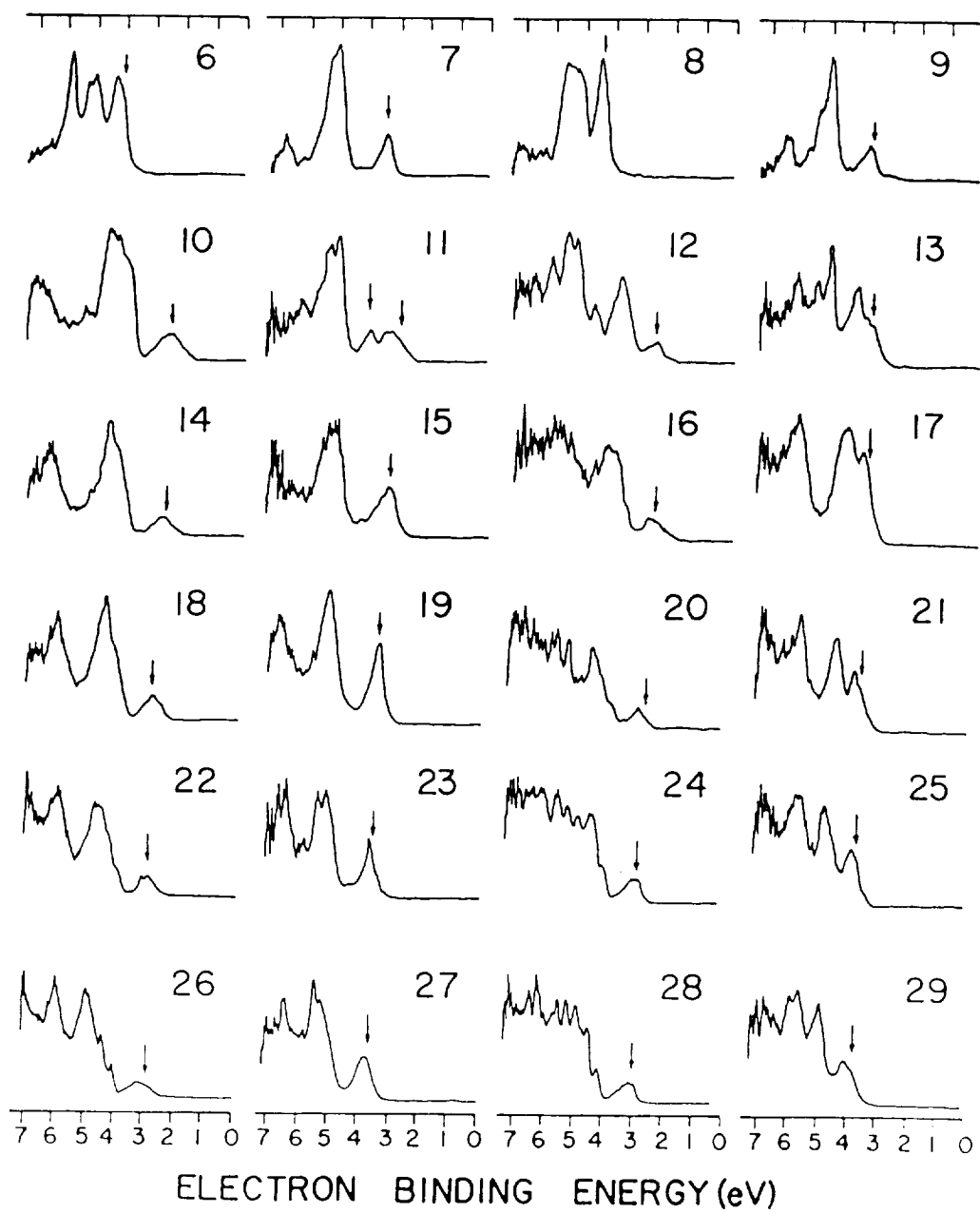
Figure 7.– UPS of negative carbon clusters in the 6-29 atom region.
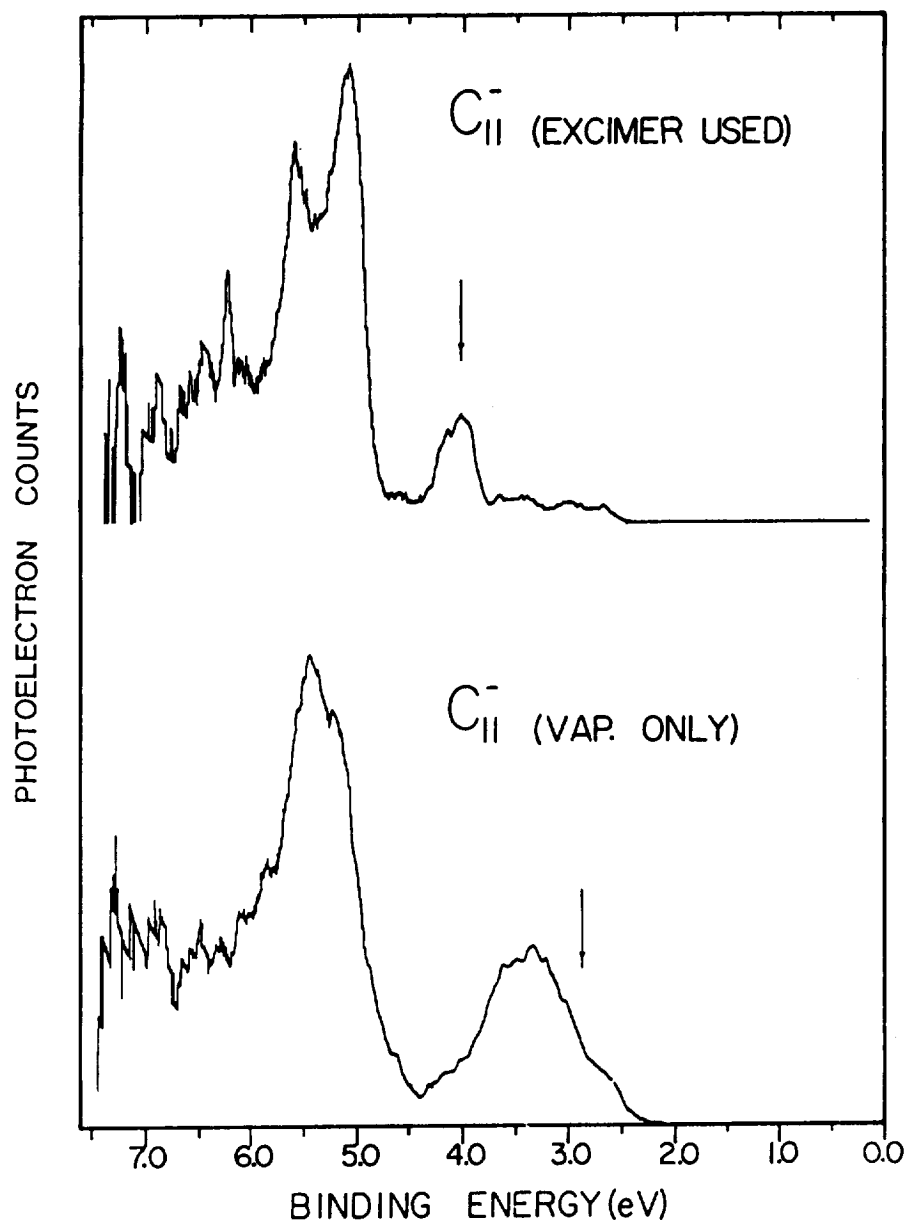
Figure 8.– UPS of C_{11}^- under two conditions which favor different geometrical forms of the cluster.
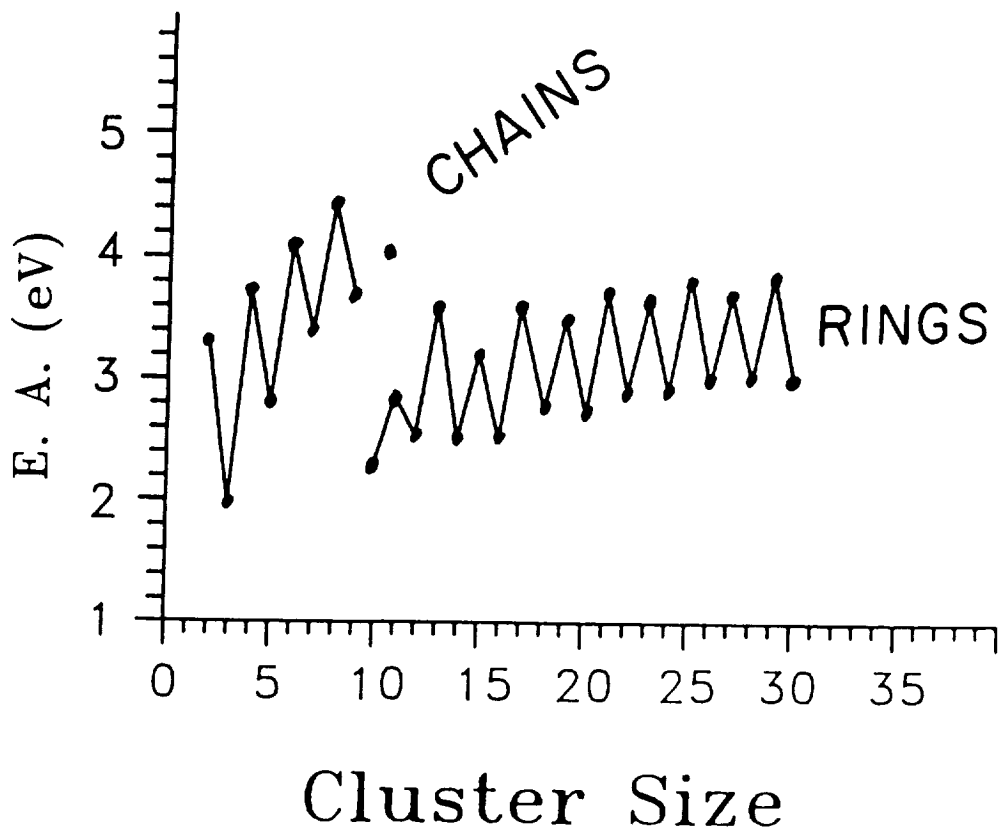
Figure 9.– Electron Affinity of carbon clusters in 2-29 region. The measured values were taken from the estimated photodetachment thresholds in the UPS data of Figs. 5-7. Note there are two values plotted for C_{11}.
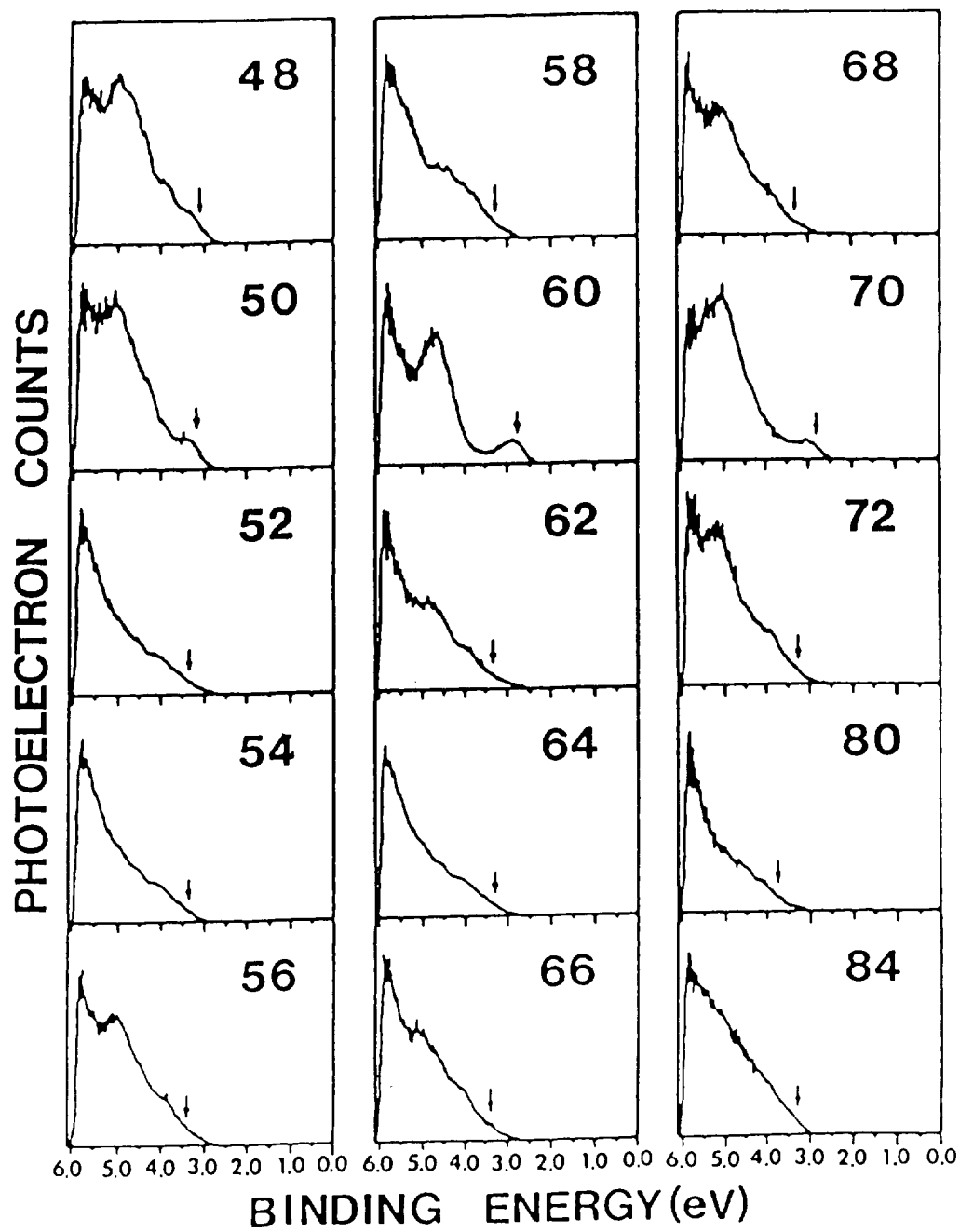
Figure 10.– Carbon cluster UPS in the 48-84 size range taken with an ArF excimer laser (6.4 eV).

C_{60}^{-} UPS

LUMO $= \underline{\mp} =$ t_{1g} t_{1u}

HOMO ++ ++ ++ ++ ++ h_u

++ ++ ++ ++ ++ ++ ++ ++ ++ ++ g_g h_g

++ ++ ++ ++ g_u

ELECTRON BINDING ENERGY (eV)
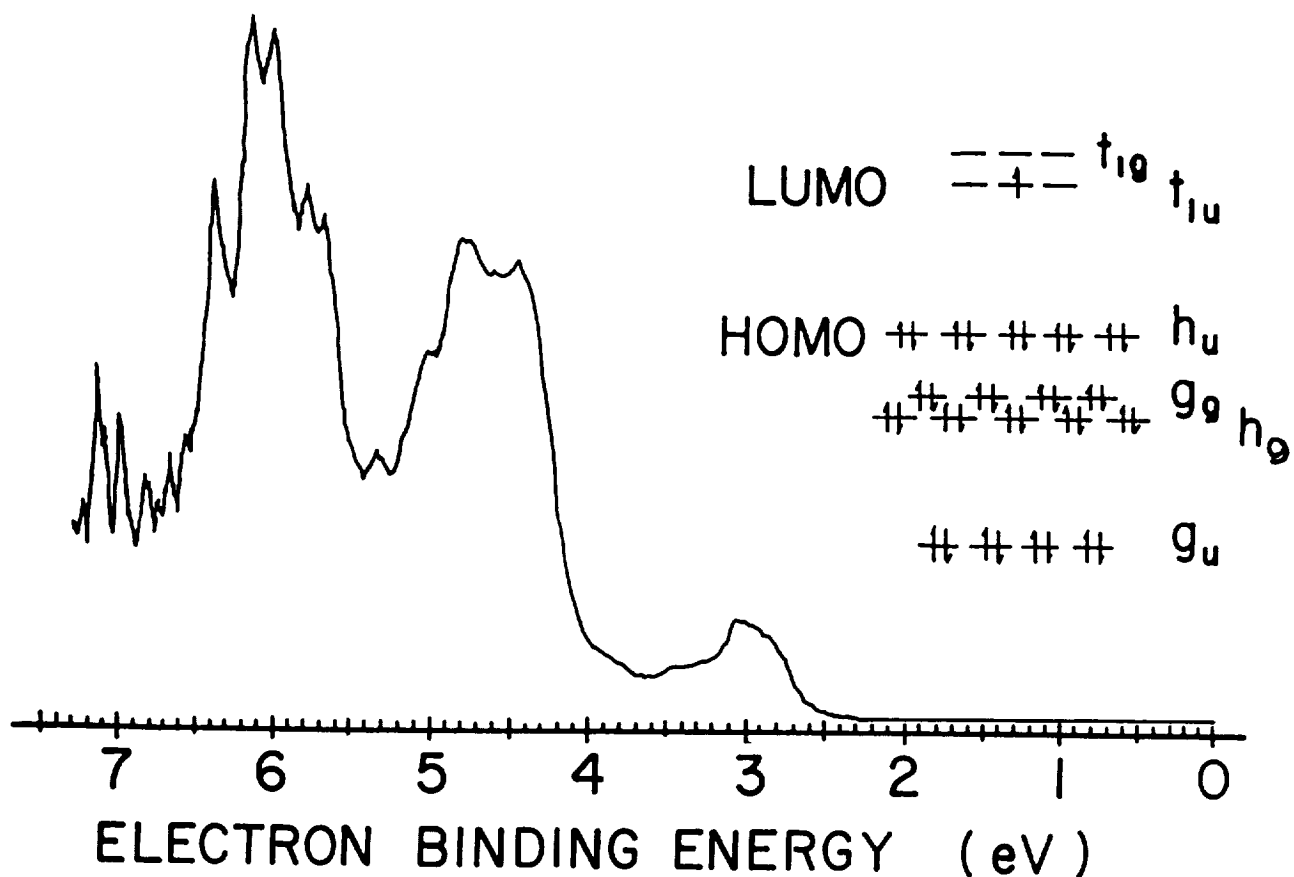
Figure 11.– C_{60}^{-} UPS taken with a F_2 excimer laser. The right side of the figure shows an approximate molecular orbital diagram for C_{60} assuming a truncated icosahedral (buckminsterfullerene) structure.
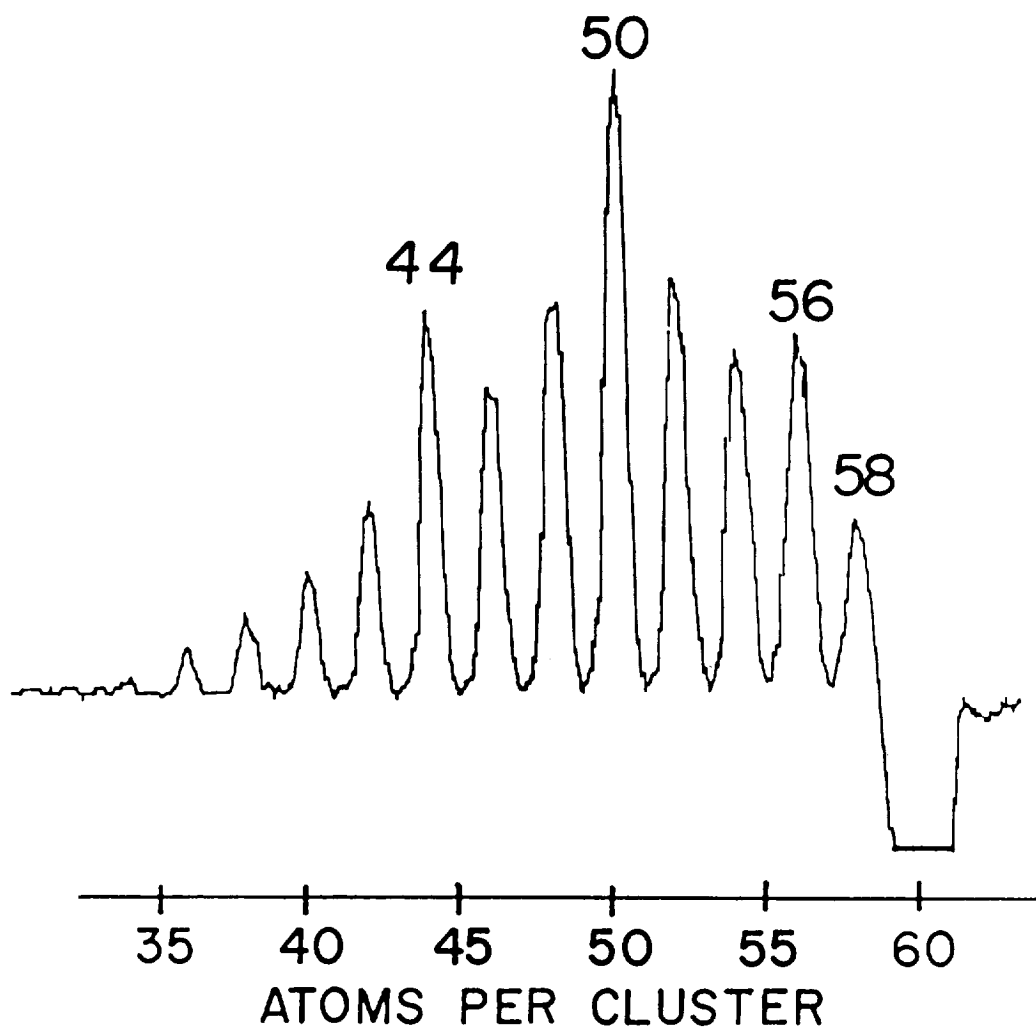
Figure 12.– C_{60}^{+} photofragmentation showing C_2 loss to produce first C_{58}^{+}, then C_{56}^{+}, etc. These data were obtained by mass-selecting C_{60}^{+} with an initial TOF mass spectrometer, and analyzing the parent and product ions with a second TOF mass spectrometer.
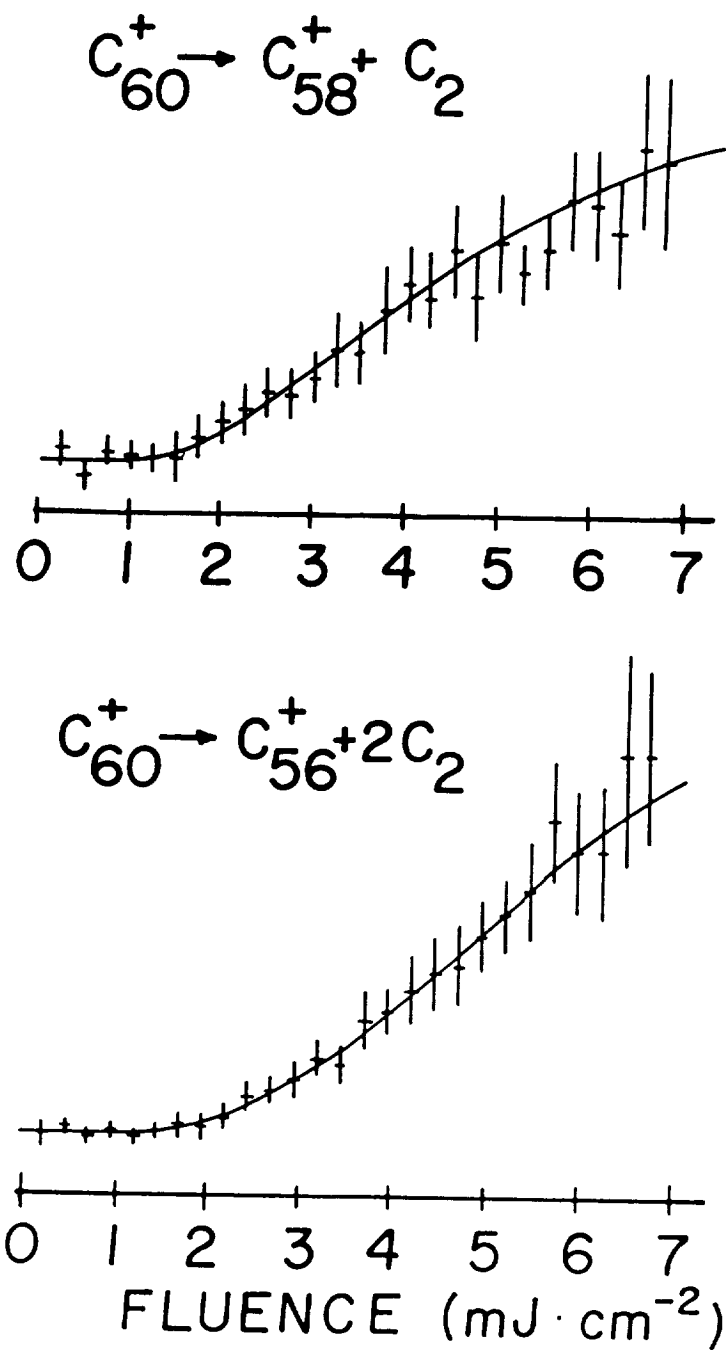
Figure 13.– Laser fluence dependence of C_{58}^+ and C_{56}^+ daughter ions fragmented from an initially mass-selected C_{60}^+ using a single shot of the 1930 Å (6.4 eV) Arf excimer laser.

ATOMS PER CLUSTER
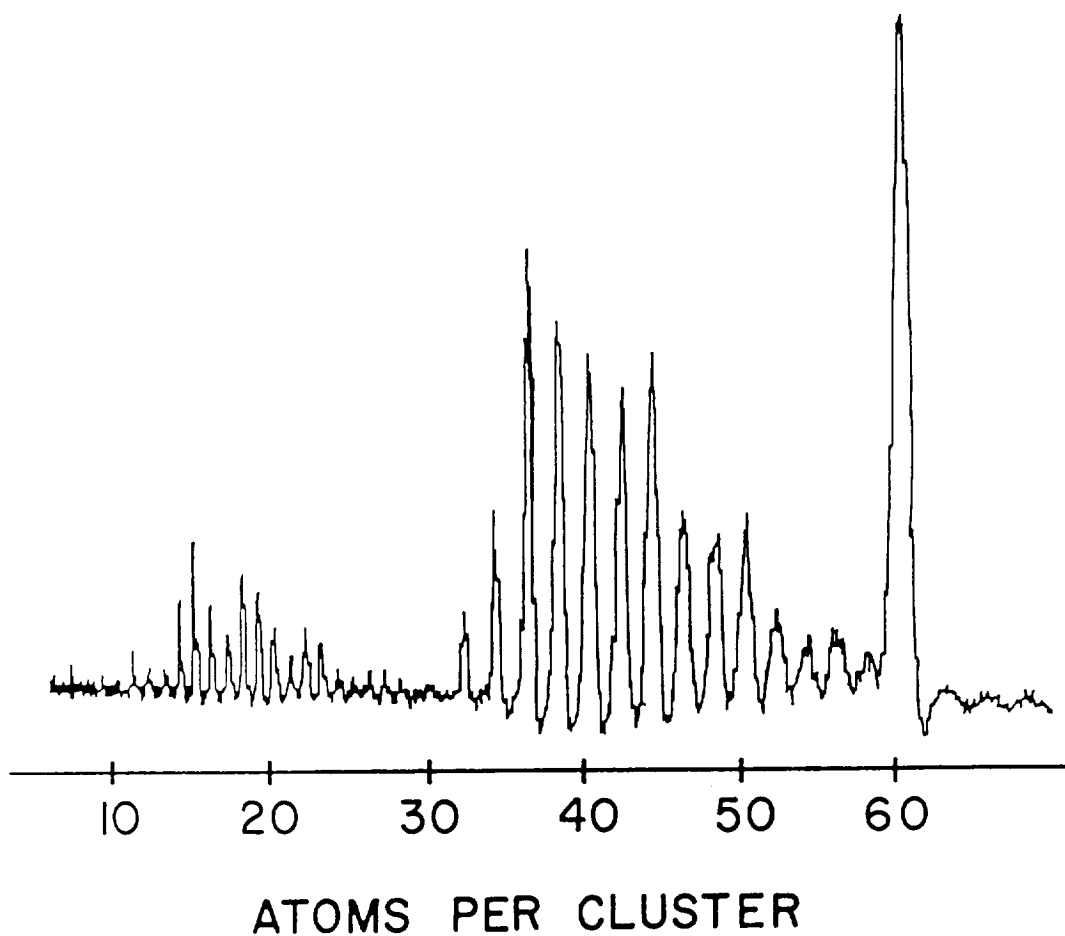
Figure 14.– Photofragmentation pattern for very highly excited C_{60}^+ showing high-order granddaughter fragments. Note the abrupt breakoff in the C_2 loss process at C_{32}^+. This is believed to be the smallest viable fullerene.
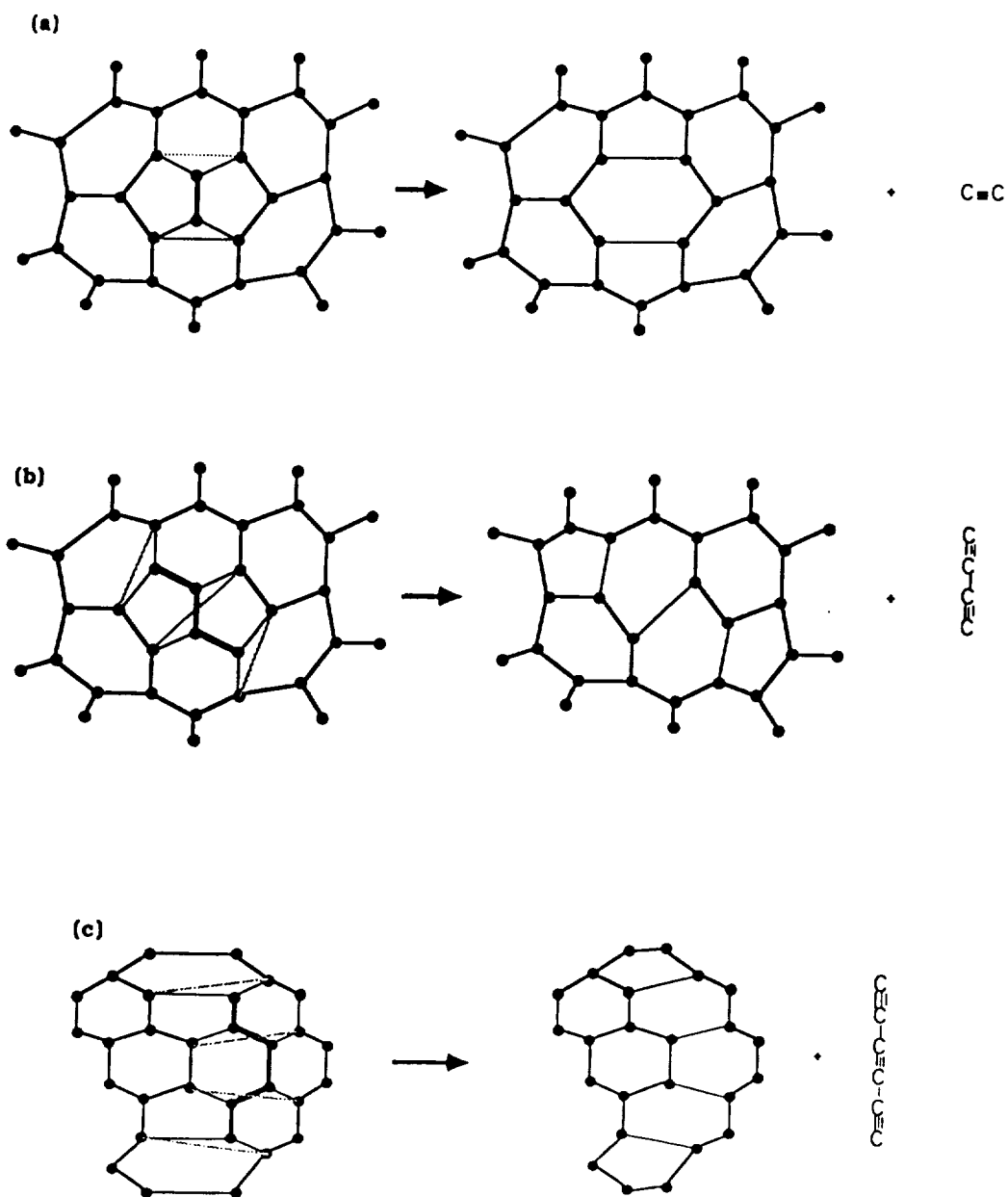
Figure 15.– Concerted fragmentation mechanism postulated to be responsible for (TOP panel) the C_2 loss from a closed fullerene net upon intense laser excitation. The middle and bottom panels depict higher-order concerted mechanisms which result in the loss of successively longer even-numbered carbon chains from the closed net. Note that all of these processes conserve the number of pentagons in the net. In contrast, all open nets, chains, and rings are expected to fragment by the loss of C_3.
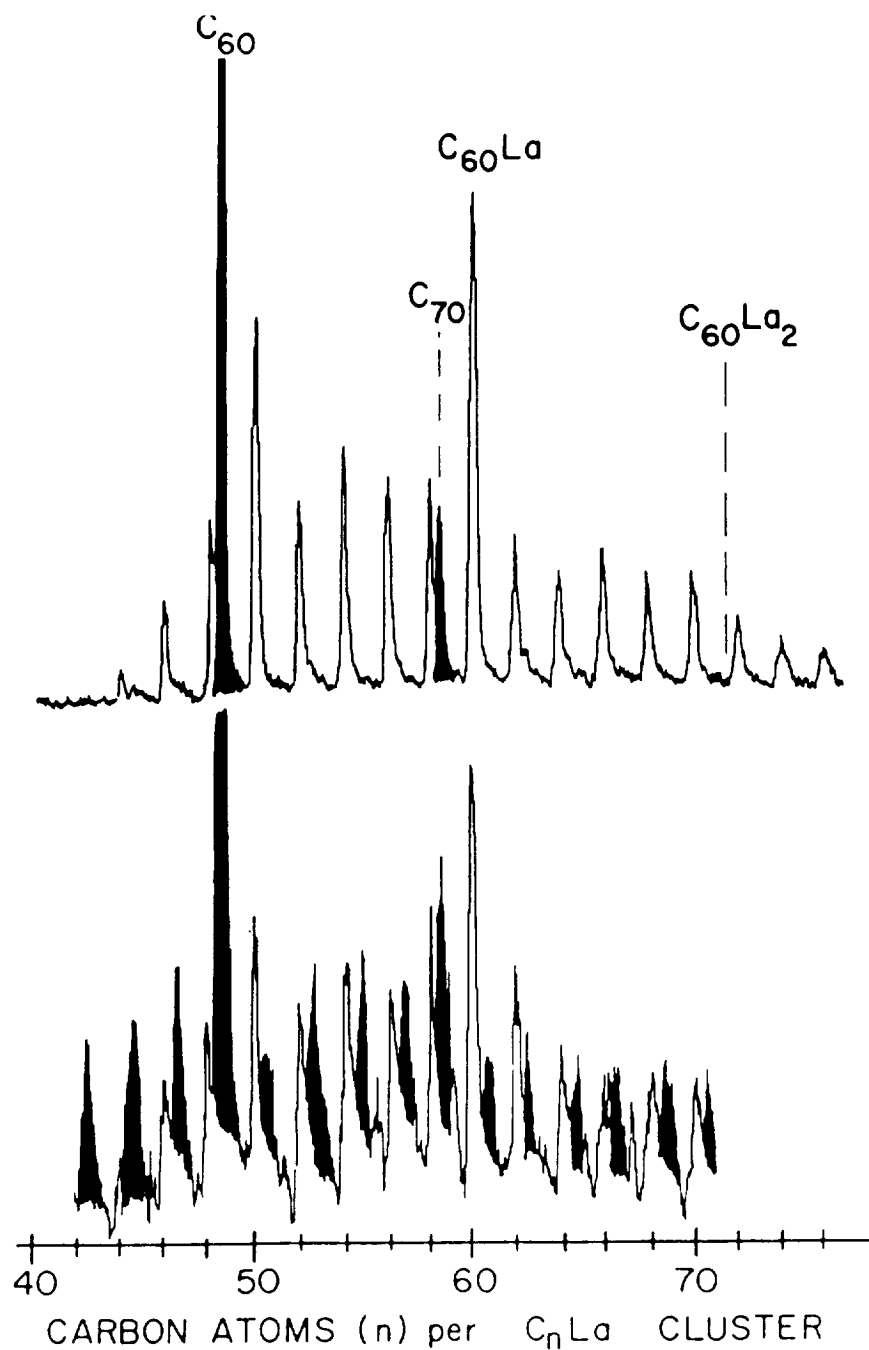
Figure 16.– TOF mass spectrum of C_nLa^+ cluster complexes (open peaks) and C_n^+ bare fullerene clusters (blackened peaks) produced by laser vaporization of a $LaCl_3^-$ impregnated graphite disk in a pulsed supersonic nozzle, followed by ionization with an ArF excimer laser as the neutral clusters passed through the TOF spectrometer. The bottom spectrum was taken at low ArF laser fluence (<0.01 mj cm^{-2}) much of an extensive unresolved baseline due to dissociating metastable ions has been subtracted here. The top spectrum was taken with an intense ArF excimer (1-2 mj cm^{-2}) sufficient to dissociate all weakly bound complexes.

241
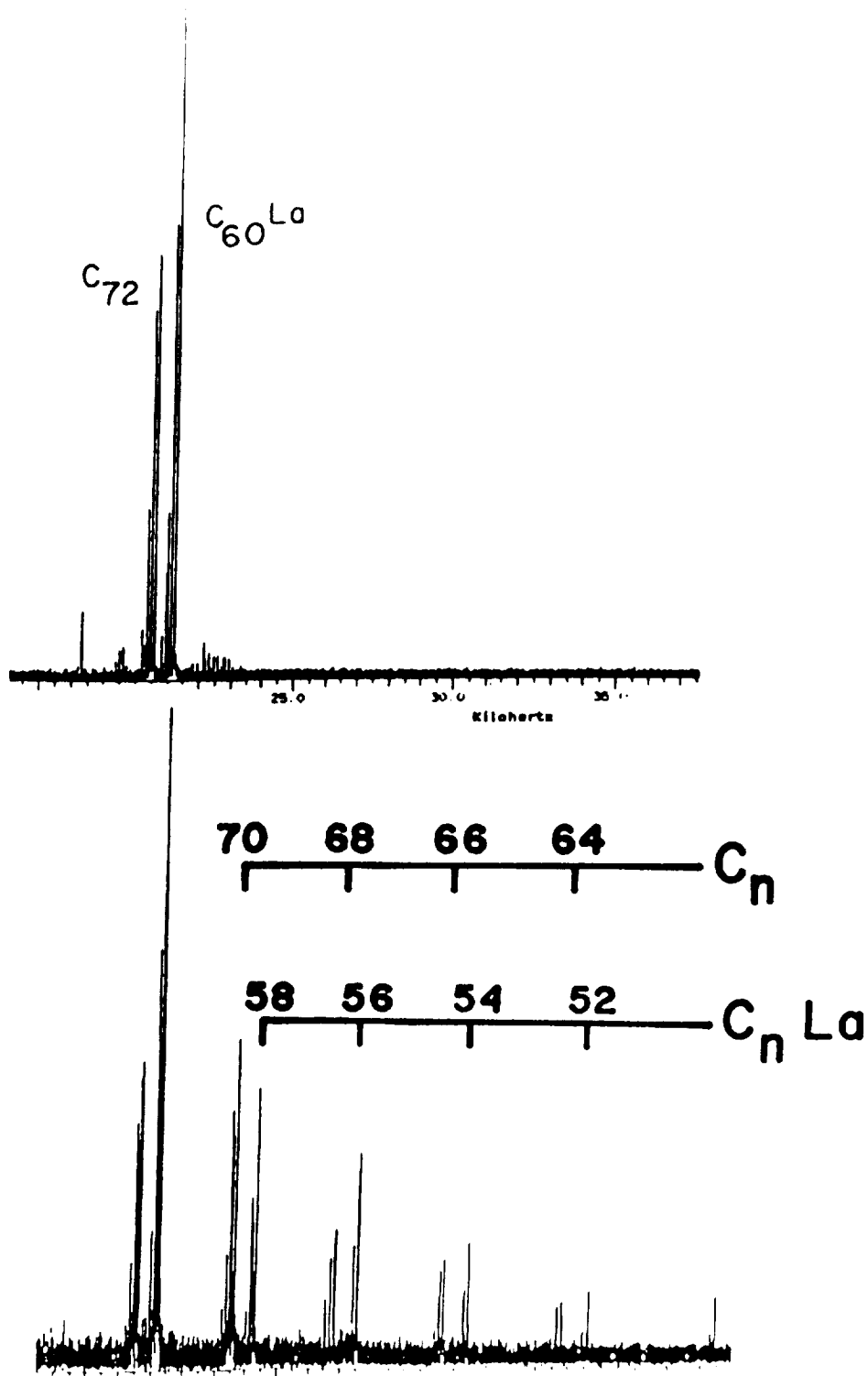
Figure 17.— ArF excimer laser photolysis experiment on C_{72}^+ and $C_{60}La^+$ trapped in an ion cyclotron resonance cell by the combination of a 6 tesla magnetic field and a weak electrostatic saddle potential. The top trace shows the Fourier transform mass spectrum before irradiation. The bottom shows the results of 50 shots of an ArF excimer laser operating at 10 Hz with a pulse fluence in the ICR cell of 4 mj cm^{-2} per shot. Note that the fragmentation mechanism of $C_{60}La^+$ is the same as that of all the bare fullerenes: C_2 loss.

$C_{60} \cdot C_6H_6$

$C_{60} \cdot CH_2Cl_2$

3830   3840   3850   3860   3870   3880
WAVELENGTH ($\overset{\circ}{A}$)
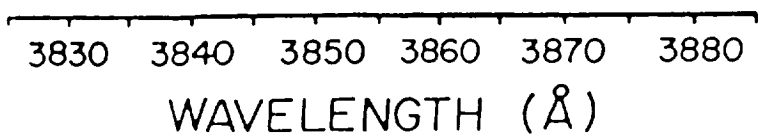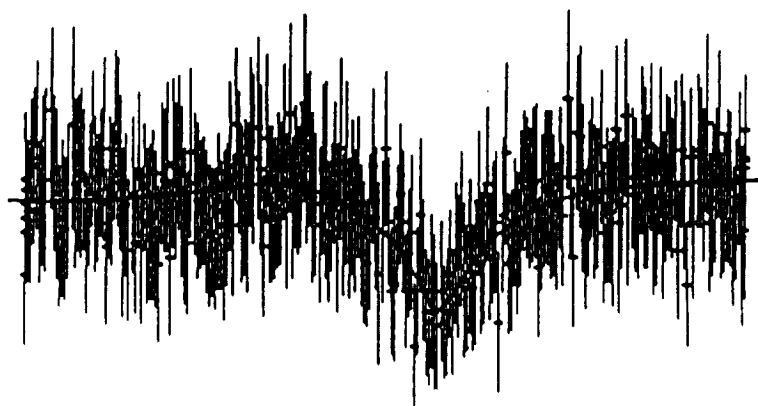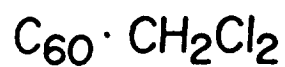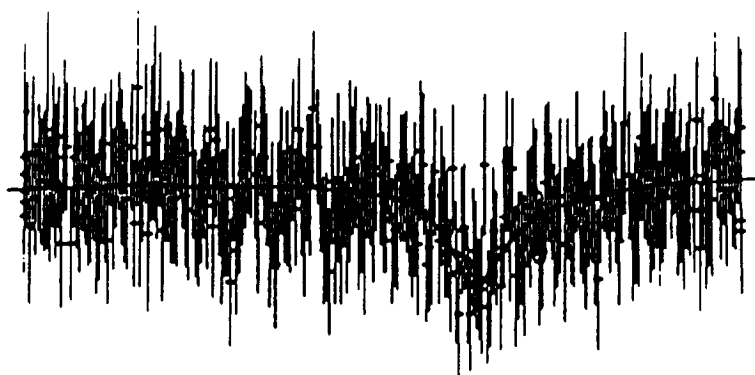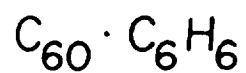
Figure 18.– Spectrum of C_{60} van der Waals complexes prepared and cooled in a supersonic beam, showing an isolated absorption band near 3860 Å.
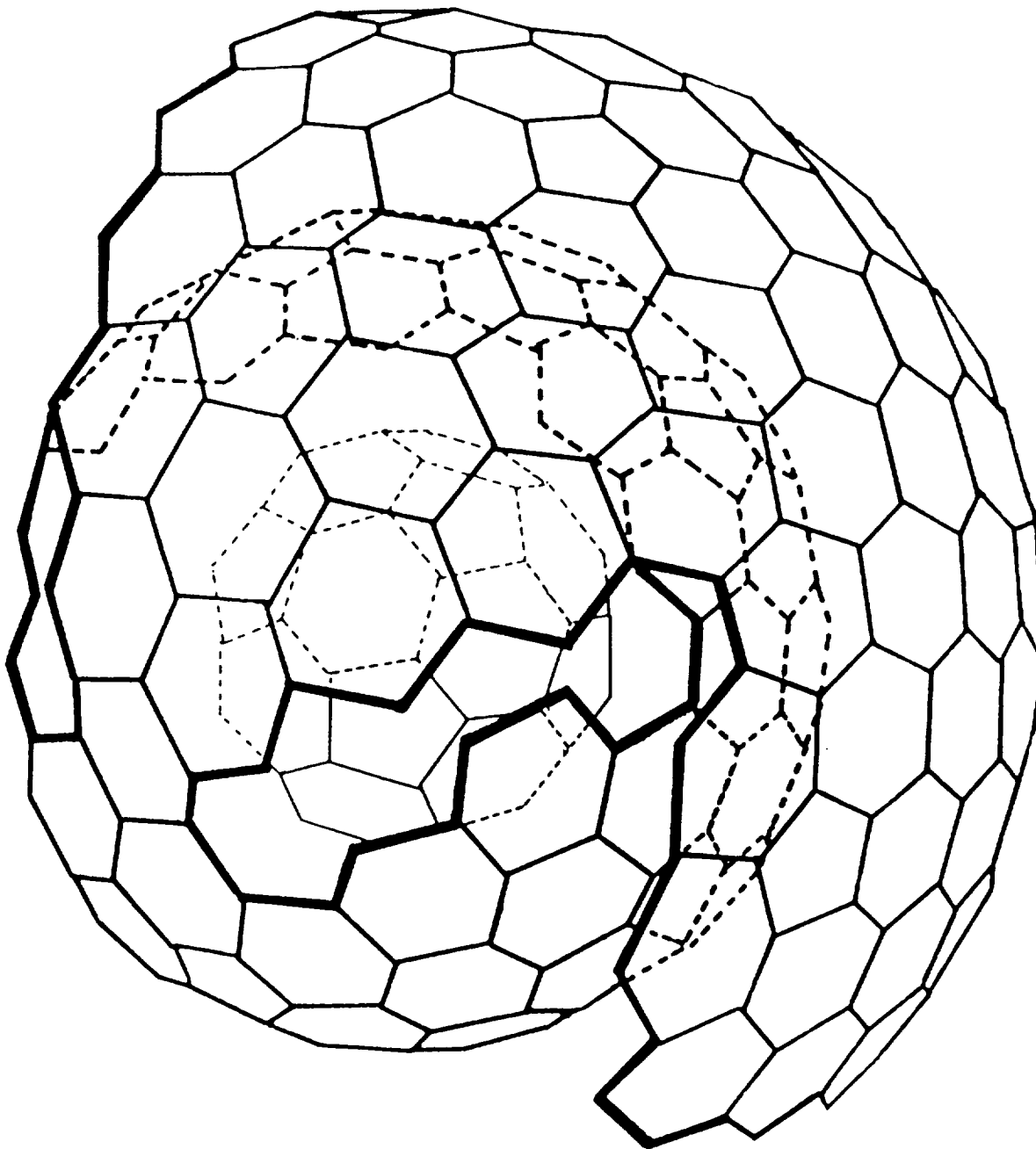
Figure 19.– Spiral carbon network structure believed to be a reasonable model for a growing carbon grain. Growth is thought to proceed from an original small carbon net which curls by the incorporation of pentagons so as to minimize dangling bonds.